



Iodine oxoacids and their roles in sub-3 nanometer particle growth in polluted urban environments

Ying Zhang^{1,2,3,*}, Duzitian Li^{2,3,*}, Xu-Cheng He^{4,5}, Wei Nie^{2,3}, Chenjuan Deng⁶,

Runlong Cai⁴, Yuliang Liu^{2,3}, Yishuo Guo¹, Chong Liu^{2,3}, Yiran Li⁶, Liangduo Chen^{2,3},
5 Yuanyuan Li^{2,3}, Chenjie Hua¹, Tingyu Liu¹, Zongcheng Wang¹, Lei Wang^{2,3}, Tuukka
Petäjä⁴, Federico Bianchi⁴, Ximeng Qi^{2,3}, Xuguang Chi^{2,3}, Pauli Paasonen⁴, Yongchun
Liu¹, Chao Yan^{2,3}, Jingkun Jiang⁶, Aijun Ding^{2,3}, Markku Kulmala^{1,2,3,4}

¹Aerosol and Haze Laboratory, Beijing Advanced Innovation Center for Soft Matter Science and Engineering, Beijing University of Chemical Technology, Beijing, China

10 ²Joint International Research Laboratory of Atmospheric and Earth System Sciences, School of Atmospheric Sciences, Nanjing University, Nanjing, China

³Jiangsu Provincial Collaborative Innovation Center of Climate Change, Nanjing, China

⁴Institute for Atmospheric and Earth System/Physics, Faculty of Science, University of Helsinki, Helsinki, Finland

15 ⁵Finnish Meteorological Institute, Helsinki, Finland

⁶State Key Joint Laboratory of Environment Simulation and Pollution Control, State Environmental Protection Key Laboratory of Sources and Control of Air Pollution Complex, School of Environment, Tsinghua University, Beijing, China

20 *These authors contributed equally to this work.

Correspondence to: Xu-Cheng He (xucheng.he@helsinki.fi) and Wei Nie (niewei@nju.edu.cn)

Abstract. New particle formation processes contribute significantly to the number concentration of
25 ultrafine particles (UFP), and have great impacts on human health and global climate. Iodine oxoacids
(HIO_x, including iodic acid, HIO₃ and iodous acid, HIO₂) have been observed in pristine regions and
proved to dominate NPF events at some sites. However, the knowledge of HIO_x in polluted urban areas
is rather limited. Here, we conducted a long-term comprehensive observation of gaseous iodine oxoacids
and sulfuric acid in Beijing from January 2019 to October 2021 and also in Nanjing from March 2019 to
30 February 2020, and investigated the contribution of HIO_x to UFP number concentration in urban
environments. HIO₃ concentration is highest in summer, up to 2.85×10⁶ cm⁻³ and 2.78×10⁶ cm⁻³ in
Beijing and Nanjing, respectively, and is lowest in winter, with a more prominent seasonal variation than
H₂SO₄. HIO₃ concentration shows a clear diurnal pattern at both sites with a daily maximum at around



noontime, similar to the atmospheric temperature, radiation and ozone (O_3) levels. HIO_2 concentration
35 has the same diurnal and seasonal trend as HIO_3 but is overall about one order of magnitude lower than
 HIO_3 concentration. Back trajectory analysis suggests that the sources for inland iodine species could be
a mix of marine and terrestrial origins, both having peak iodine emission in warm seasons. While the
contribution of HIO_2 to particle growth is marginal in Beijing and Nanjing, our results demonstrate that
 HIO_3 enhances the particle survival probability of sub-3 nm particles by about 40% (median) and
40 occasionally by more than 100% in NPF events, suggesting HIO_x are non-negligible contributor to UFPs
in polluted urban areas. As the growth contribution from HIO_3 and H_2SO_4 is similar on a per-molecule
basis, we propose that the sum of HIO_3 and H_2SO_4 could be used to estimate sub-3 nm particle growth
of inorganic acid origin, in the polluted atmospheres with a significant amount of HIO_x .

1 Introduction

45 Aerosol particles are ubiquitous in Earth's atmosphere and have both primary and secondary sources
(Kulmala et al., 2004b). Primary aerosol emissions include natural sources including the emission of sea
spray, release of soil mineral dust, emission of biomass burning smoke, and the injection of volcanic
debris (Claudio Tomasi, 2017) and anthropogenic emissions such as fuel combustion, industrial
processes and transportation (Claudio Tomasi, 2017). Besides direct emissions, atmospheric new particle
50 formation (NPF), a secondary particle source, plays a significant role in increasing aerosol population
(Kulmala et al., 2012). Only a few vapours, such as sulfuric acid (H_2SO_4), water vapour (H_2O), ammonia
(NH_3), amines (e.g., dimethylamine, C_2H_7N) and highly oxygenated organic molecules (HOMs), are
widely confirmed to nucleate and form new particles under atmospheric conditions (Kulmala et al.,
2004a; Kürten et al., 2016; Li et al., 2020; Yao et al., 2018; Almeida et al., 2013; Kirkby et al., 2011;
55 Kirkby et al., 2016; Lehtipalo et al., 2018; Tröstl et al., 2016). Once growing past the critical sizes (e.g.,
50 nm to 100 nm), these newly formed particles can be activated as cloud condensation nuclei (CCN),
which in turn influence cloud formation and have climatic effects (Kerminen et al., 2005). Additionally,
NPF is a dominant source of atmospheric ultrafine particles in polluted urban environments (Yan et al.,
2021). These small particles (< 50 nm) can penetrate into the respiratory system, thus posing health risks
60 to human beings (Chen et al., 2016; Downward et al., 2018). Therefore, understanding NPF processes is



important both in terms of predicting climate change and understanding the health risks of aerosols (Kulmala et al., 2022).

Due to its chemically complex nature, the understanding of the key precursor vapours and controlling mechanisms of urban NPF is still limited. Gaseous sulfuric acid and dimethylamine (DMA, C_2H_7N) are believed to play important roles in aerosol nucleation in urban environments (Xiao et al., 2021; Yao et al., 2018; Cai et al., 2021d; Almeida et al., 2013; Cai et al., 2022b). A recent study quantitatively demonstrated the decisive role of H_2SO_4 in initiating nucleation with the presence of stabilisers such as amines and NH_3 in Beijing (Yan et al., 2021). The subsequent growth of fresh particles is contributed both by H_2SO_4 and oxidised organic vapours depending on the particle sizes. In urban Beijing, it was suggested that H_2SO_4 and its clusters contribute significantly to the growth of 1.5-3 nm particles (Deng et al., 2020b) while gas-phase oxygenated organic molecules (OOMs) promote the growth of 3-25 nm particles (Qiao et al., 2021).

Besides these widely studied species, oxidized iodine compounds were also found to introduce rapid particle formation, mostly observed in mid-latitude coastal sites (Hoffmann et al., 2001; Mäkelä, 2002; O'dowd et al., 2002). Iodine nucleation was conventionally thought to be initiated by iodine oxides (Jimenez, 2003; Gomez Martin et al., 2020; O'dowd and Hoffmann, 2005; Hoffmann et al., 2001; O'dowd et al., 2002). However, field observations at the Mace Head observatory and dedicated experiments carried out in the CLOUD chamber at CERN revealed iodine oxoacids (HIO_x , i.e., HIO_3 and HIO_2 in this study) as the key nucleating species in pristine regions (Zhang et al., 2022; He et al., 2021b). With state-of-the-art mass spectrometric methods, iodine oxoacids were recently identified in locations other than mid-latitude coastal sites, such as in Arctic sites (Sipilä et al., 2016; Baccarini et al., 2020; Beck et al., 2021; He et al., 2021b), Antarctica sites (Jokinen et al., 2018; He et al., 2021b), boreal forest sites (Jokinen et al., 2022; He et al., 2021b), a remote marine site (He et al., 2021b) and importantly also in polluted urban sites (He et al., 2021b). Chamber experiments have shown that HIO_3 (with HIO_2) nucleates faster than H_2SO_4 with 100 pptv NH_3 at the same temperature and equal acid concentrations, although iodine oxoacid nucleation rates are still lower than H_2SO_4 -DMA nucleation (He et al., 2021b). It is worthwhile to note that the nucleation involving both iodine oxoacids and DMA remains unclear and iodine oxoacid nucleation may further be enhanced by strong bases (e.g., different amines) in urban environments. After the formation of fresh particles, HIO_3 dominates the growth of iodine particles



between 1.8 and 3.2 nm at growth rates equal to those of H₂SO₄ (He et al., 2021b). It can be expected that, iodine oxoacids will contribute at least to sub-3 nm particle growth, and potentially also to particle nucleation, in polluted urban environments. Therefore, iodine oxoacids have the potential to enhance the survival probability (Kulmala et al., 2017) of fresh particles in the urban environment.

95

In order to quantitatively understand the contribution of iodine oxoacids in urban particle formation, we conducted a long-term measurement of iodine oxoacids and sulfuric acid (H₂SO₄) in urban Beijing from 2019 to 2021, and in suburban Nanjing from March 2019 to February 2020. Diurnal and seasonal trends of iodine and sulfur oxoacids are analysed and the potential sources of the unexpected iodine oxoacids are discussed. Moreover, we quantitatively discuss the contribution of HIO₃ to aerosol growth rate below 3 nm (GR_{<3nm}) and the potential enhancement in particle survival probability. Our study provides the first long-term observations of iodine oxoacids in polluted urban environments which could contribute to aerosol formation studies in inland cities.

100

2 Methods

2.1 Measurement sites and instruments

105

2.1.1 Sites

110

115

The measurement in urban Beijing was conducted from January 2019 to October 2021. The site locates on the fifth floor of the teaching building at the west campus of Beijing University of Chemical Technology (Aerosol and Haze Laboratory (AHL)/BUCT station, 39 ° 56'N, 116 ° 17'E). Located about 150 km away from the nearest coastline in the southeast, the station is surrounded by residential buildings and three main roads and a detailed description of this site can be found in a previous study (Liu et al., 2020). The observations in Nanjing were conducted at the Station for Observing Regional Process of Earth System (SORPES; 118°57'E, 32°07'N), a research and experiment platform inside Nanjing University, Xianlin Campus, 20 km northeast of downtown Nanjing and about 190 km away from the nearest coastline in the east. Because of its unique geophysical location, the SORPES is considered to be a regional background station under the influence of anthropogenic plume from YRD (Yangtze River Delta) city cluster and multiscale transport coupled with Asian monsoon (Ding et al., 2016).



2.1.2 Acid concentrations

Gaseous iodine oxoacids (HIO_3 and HIO_2) and H_2SO_4 were detected by the nitrate-CIMS (Aerodyne
120 Research Inc. and ToFwerk AG) composed of a chemical ionization (CI) source and an atmospheric
pressure interface time-of-flight mass spectrometer (API-TOF). Two long time-of-flight mass analysers
(LToF, resolution at around 10,000 Th Th^{-1}) were used at the AHL/BUCT station from January 2019 to
October 2021 and at SORPES station from March 2019 to December 2019, respectively, while a lower
resolution time-of-flight analyser (HToF, resolution at around 5,000 Th) was utilized at the SORPES
125 station from January 2020 to February 2020. As the comprehensive description of nitrate-CIMS has been
given in previous works (Junninen et al., 2010; Jokinen et al., 2012), they are only briefly discussed here.
Ambient air was drawn into a laminar flow reactor through a 0.75 in. diameter stainless steel tube with a
sample flow of about 7.2 L/min and surrounded by a purified airflow of 32 L/min serving as the sheath
flow at the AHL/BUCT station and 25 L/min at the SORPES station. The dominant reagent ions were
130 nitrate ions (NO_3^- and $\text{HNO}_3 \cdot \text{NO}_3^-$ and $\text{HNO}_3\text{HNO}_3 \cdot \text{NO}_3^-$), which were generated in the sheath flow
by exposing gaseous nitric acid in the sheath flow to a photo ionizer X-ray (Model L9491, Hamamatsu,
Japan). The data of nitrate-CIMS were acquired at 1 Hz time resolution and analysed with the MATLAB
(MathWorks Inc.) toolbox ToFTools package (version 6.11) (Junninen et al., 2010).

2.1.3 Particle number size distribution

135 The particle number size distribution (PNSD) ranging from ~1 nm to 10 μm was measured using a home-
made diethylene glycol scanning mobility particle spectrometer (DEG-SMPS, 1-4.5 nm) (Jiang et al.,
2011) equipped with the miniature cylindrical differential mobility analyser (mini-cy DMA) (Cai et al.,
2017a) and a home-made particle size distribution system (PSD, 3 nm-10 μm) (Liu et al., 2016),
respectively at AHL/BUCT station, whereas two Scanning Mobility Particle Sizers (SMPSs) equipped
140 with a TSI longDMA (TSI Inc., model 3081) and a TSI nanoDMA (TSI Inc., model 3085), respectively
and Aerodynamic Particle Sizer (APS, TSI, APS-3321, USA, 500-1000 nm) were deployed to measure
PNSD at SORPES station. Additionally, ions of sizes range from 0.8 nm to 42 nm were measured using
a Neutral cluster and Air Ion Spectrometer (NAIS, Airel Ltd., Estonia) (Manninen et al., 2016) in Nanjing.



2.1.4 O₃ concentration and other meteorological factors

145 The ozone (O₃) concentration was measured using ozone analysers (49i, Thermo Fisher Scientific Inc. USA) at both sites. Additionally, ambient meteorological factors, including temperature (T), relative humidity (RH), and ultraviolet B radiation (UVB) were measured using an Automatic Weather Station (AWS310, Vaisala Inc.) in Beijing, whereas T, RH, and downward short-wave radiation (DSR) were recorded by sensors at the height of 44 m above the ground level at the SORPES station. The T and RH
150 were measured by a temperature and relative humidity probe (HMP155A, Campbell Inc., USA), and the DSR was recorded by a CNR4 net radiometer (OTT Hydromet Corp. Germany).

2.2 Data analysis

2.2.1 Characteristic of NPF events from PNSD

According to a widely used method (Kulmala et al., 2012), we classified all of the measurement days
155 into NPF and non-NPF events at both sites. All undefined days were regarded as non-NPF events in this study. Since there were periods when some key instruments failed to work, the NPF frequencies in each month were calculated as the ratio of the NPF event days to the days with valid data. The monthly statistics at both sites were summarized in Table S1. From the measured particle number size distribution, we calculated the condensation sink (CS) (Laakso et al., 2004; Kulmala et al., 2012), coagulation sink
160 (CoagS) (Kulmala et al., 2001), and growth rate (GR) for the NPF events.

CS, which characterises the loss rate of gaseous precursors and clusters onto the particles (Lehtinen et al., 2003) was calculated using the equation Eq. (1) (Kulmala et al., 2012):

$$165 \quad CS = 4\pi D \sum_j \frac{1}{2} d_{p,j} \beta_m(Kn_j, \alpha) N_j, \quad (1)$$

where, D is the H₂SO₄ vapour diffusion coefficient; $d_{p,j}$ is particle diameter; β_m is transitional correction factor for mass flux as a function of Kn_j (Knudsen number) and α (mass accommodation coefficient, assumed to be unity in this work) as shown in Eq. (2); N_j is the number concentration of
170 $d_{p,j}$, and the particle diameter is corrected for growth factor according to T and RH (Laakso et al., 2004).



$$\beta_m = \frac{1+Kn_j}{1+0.377Kn_j+1.33Kn_j(1+Kn_j)/\alpha}, \quad (2)$$

To quantify if notable growth is to occur, especially at sizes below a few nanometers, it is crucial to understand the loss process of fresh particles. Coagulation scavenging of freshly formed particles into pre-existing particles before growing to significant sizes is essential for estimating the concentration of newly nucleated particles at the size of 1.5-2 nm (Kulmala et al., 2001). Aerosol coagulation sink (CoagS) represents this kind of coagulated scavenging characteristics. CoagS (the loss through coagulation among particles) was determined from Eq. (3). Here, K_{ij} is the coagulation coefficient (Kulmala et al., 2001).

180

$$CoagS = \sum_j K_{ij}N_j, \quad (3)$$

Besides, the GRs in NPF events were determined with both the appearance time method (including APT- x and APT- y) and the mode fitting method (MOD) to minimize the uncertainty from calculations (Kulmala et al., 2012; Dada et al., 2020). Detailed approach is shown in supplementary materials. The size-segregated GRs were calculated in two size ranges, i.e., sub-3 nm (GR_{<3}) and 3-7 nm (GR₃₋₇) based on the appearance time method, and the 50% appearance time is fitted by smoothing the normalized concentration timeseries for the particle of each size bin (Lehtipalo et al., 2014; He et al., 2021a). After determining the 50% appearance time for each size bin, the GRs were fitted using the linear least square method both with time as x and y to compare with each other and minimize the error. They are referred to as APT- x and APT- y , respectively in this study. The slope of particle size to their 50% appearance time was regarded as GR using APT- x , which is the traditional way. However, as the particle diameter is exactly measured by our instruments and the 50% appearance time is the independent variable determined by calculations, we also tried to use the latter as the independent variable to fit the GR. In this case, the GR was determined as the inverse of the fitted slope. The mode fitting (MOD) method fits the particle number size distribution to find the mode diameters at any given time and tracks the evolution of particle sizes. Up to now, there is still a debate about whether to adopt the appearance time method or the mode fitting method for GR calculation, as neither is perfect for calculating GR for ambient observations (Qiao et al., 2021; Deng et al., 2020b). For example, it is difficult to define the accurate mode diameter, especially for sub-3 nm particles when the new particle formation just occurs. Therefore,

200



there could be some underestimation while using mode fitting method to calculate $GR_{<3}$ (Cai et al., 2022a). Determining the sub-3 nm particle growth can also be difficult for the 50% appearance time method for similar reasons. Additionally, appearance time method might be more sensitive to other processes as it does not track the growth of a particle or a population. (Lehtipalo et al., 2014; Cai et al., 2021c; He et al., 2021a). In this study, we report results using both methods to reduce the overall uncertainty of GR calculation and to provide a confidence range of GR. In both cases, the GR is determined from the rate of change in diameter shown as Eq. (4) (Kulmala et al., 2012).

$$GR = \frac{dd_p}{dt}, \quad (4)$$

210

It is worthwhile to note that we corrected the GR obtained from the 50% appearance time method for the impact of coagulation sink, following Eq. (5) (Cai et al., 2021c).

$$GR_{corr,cond} = GR_{conv} - \left(CoagS + \frac{CoagSrc}{2N_p} \right) \times \left[\sqrt[3]{(d_p^3 + d_1^3)} - d_p \right] - GR_{coag}, \quad (5)$$

215

where the GR_{conv} is the GR calculated from conventional appearance time method in $\text{nm}\cdot\text{s}^{-1}$; $CoagSrc$ is the coagulation source defined as the production rate of the particle size bin because of coagulation, $\text{cm}^{-3}\cdot\text{s}^{-1}$, calculated using the Eq. (6); N_p is the number concentration of particles with the size d_p ; GR_{coag} is the coagulation growth rate in $\text{nm}\cdot\text{s}^{-1}$ from Eq. (7). More specific details can be found in Cai et al. (2021c).

220

$$CoagSrc = 0.5 \times \iint_{d_{p,1}^3 \leq d_i^3 + d_j^3 \leq d_{p,u}^3} \beta_{i,j} n_i n_j \times d \log d_i \times d \log d_j, \quad (6)$$

$$GR_{coag} = \sum_{d_p=d_{min}}^{d_p=d_p} \left\{ \beta_{p,i} N_i \times \left[\sqrt[3]{(d_p^3 + d_i^3)} - d_p \right] \right\}, \quad (7)$$

225 The counterbalance of CoagS and GR considerably affects the survival of small clusters. Survival probability (SP) is utilized to quantify the competition between growth and scavenging mentioned above (Veli-Matti Kerminen, 2002; Kerminen et al., 2005). We defined the $SP_{1.5-3}$ and SP_{3-7} as the likelihood that the particles can grow from the smaller sizes to the larger sizes (i.e., from 1.5 to 3 nm and from 3 to



7 nm, respectively) before they are scavenged by coagulation. The SP can be calculated following Eq.
 230 (8) (Lehtinen et al., 2007).

$$SP = \exp \left\{ \frac{d_{p1}}{m-1} \frac{CoagS}{GR} \left[\left(\frac{d_{p2}}{d_{p1}} \right)^{1-m} - 1 \right] \right\}, \quad (8)$$

where d_{p1} and d_{p2} are the lower limit size and upper limit size, respectively; CoagS is the coagulation
 235 sink at the lower limit size; GR is the averaged growth rate in the size range, from both corrected
 appearance time method and mode fitting method; m was assumed to be 1.7 according to the measured
 PNSDs (Lehtinen et al., 2007).

2.2.2 Contribution of HIO₃ to GR and SP

240 The particle growth rate due to HIO₃ concentration was observed to be linear in the CLOUD experiment,
 shown as Eq. (9), which is fitted at 10 °C (He et al., 2021b):

$$GR(\text{HIO}_3)_{1.8-3.2} = 10^{\log_{10}[\text{HIO}_3]-6.75}, \quad (9)$$

where [HIO₃] is the iodic acid concentration in molecules cm⁻³ and $GR(\text{HIO}_3)_{1.8-3.2}$ is the growth rate
 of 1.8 to 3.2 nm particles in nm h⁻¹. However, the size range of sub-3 nm particles used in this study (1.5
 245 to 3 nm) slightly differs from 1.8 to 3.2 nm and this formulation does not provide the growth rates of 3
 to 7 nm particles. Additionally, as the temperature in summer seasons in both Beijing and Nanjing
 (around 22 to 36 °C) is much higher than 10 °C, additional temperature correction is needed. In this study,
 we adopt the equation provided by Nieminen et al. (2010) for these corrections:

$$250 \quad GR(\text{HIO}_3) = \frac{\Delta d_p}{\Delta t} = \frac{\Delta d_p \text{HIO}_3 \alpha_m m v}{2 \rho_v d_p} \cdot \sqrt{\frac{8kT}{\pi m v}} \cdot \frac{1}{\left[\frac{2x_1+1}{x_1(x_1+1)} - \frac{2x_0+1}{x_0(x_0+1)} + 2 \ln \left(\frac{x_1(x_0+1)}{x_0(x_1+1)} \right) \right]}, \quad (10)$$

where the subscript “v” refers to HIO₃. Additionally, x_0 and x_1 are the ratios of the diameter of HIO₃
 molecule divided by the particle diameter at which the initial growth occurs (e.g., 1.5 nm or 1.8 nm) and
 particle diameter at which the particles grow to (e.g., 3 nm or 3.2 nm), respectively. Two sets of growth
 255 rates were calculated using this equation: 1) the first set utilized the measured ambient temperature at the
 given growth period of NPF events with 1.5 to 3 nm or 3 to 7 nm as the growth ranges and 2) the second



set calculated the growth rates at 10 °C with 1.8 to 3.2 nm as the growth range (the same as at CLOUD).

The ratios of the growth rates calculated by 1) and 2) therefore give the correction factors that can be applied to Eq. (9) to correct the temperature and size differences.

260 To quantify the growth rates of particles with mean diameter from around 1 nm to 7 nm in Nanjing, the negative ion number size distribution collected by NAIS was utilized. However, it is extremely difficult to use the NAIS to capture sub-3 nm particle growth rates as the limited atmospheric ions are mostly captured by larger particles in polluted urban environments and thus leaving the sub-3 nm particle growth undetectable (see supplementary materials for details). Therefore, in all NPF cases occurred at the

265 SORPES station, the contribution of gaseous iodic acid to sub-3 nm growth is only quantified by comparing its contribution with that of sulfuric acid during the same event, since H₂SO₄ is believed to be the dominant vapour for particle initial growth in sub-3 nm range (Deng et al., 2020b). H₂SO₄ contribution to GR is calculated as a first-order approximation as Eq. (11) (Stolzenburg et al., 2020), where $d_p = \frac{d_{p_{initial}} + d_{p_{final}}}{2}$ in nm and [H₂SO₄] is the gas phase H₂SO₄ concentration in molecule cm⁻³.

270

$$GR(\text{H}_2\text{SO}_4) = (2.68 \times d_p^{-1.27} + 0.81) \times ([\text{H}_2\text{SO}_4] \times 10^{-7}) , \quad (11)$$

We define SP_{tot} as the particle survival probability calculated using the measured GRs (in Beijing) or the expected growth rate considering growth contributions from both H₂SO₄ and HIO₃ (in Nanjing). In order

275 to quantify the SP enhancement by HIO₃, we further define SP₁ which represents the calculated survival probability using GRs after deducting the growth contribution from HIO₃. Therefore, the enhancement factor (EF) of SP can be represented as

$$EF = \frac{SP_{tot}}{SP_1} - 1 . \quad (12)$$

280

2.2.3 Iodic acid (HIO₃) precursor proxy

In order to investigate the source of gaseous HIO₃ at both sites, a daytime proxy formula is built to describe the precursor level of measured HIO₃, which is as follows:

$$Proxy_{pre} = \frac{[\text{HIO}_3] \times CS}{UVB} \quad (13)$$



285 Eq. (13) is derived by assuming the HIO_3 concentration to be at a pseudo-steady state (the production rate equals to the loss rate). Based on current knowledge about HIO_3 formation pathways, the proxy is not intended to elucidate the composition of species serving as HIO_3 precursor or the related reactions. Instead, it considers the photochemical reaction as the daytime formation pathway and condensation onto pre-existing aerosol particles as the only sink for gaseous HIO_3 .

290

3 Results and Discussion

3.1 Overview of the measurement

The measurement overviews in both Beijing and Nanjing are presented in Fig. 1, including the timeseries of T, O_3 , HIO_x , and H_2SO_4 concentrations, as well as the frequency of NPF events in each month. It should be noted that each point on timeseries panels refers to daytime mean value. In this work, daytime duration is defined between 08:00 and 16:00 in local time (UTC+8) considering the preferred time window of NPF events in China (Kulmala et al., 2021), as shown in Fig. S2.

In Fig.1(a)/(d), it is obvious that the seasonal patterns of T and O_3 are similar during measurement periods in both sites, i.e., both peak in the summer. The O_3 levels are roughly the same at both sites and the maximum values of daily mean T are both over 35°C , though the lowest T (about 1°C) in Nanjing is significantly higher than that in Beijing (about -12°C).

H_2SO_4 concentration is slightly lower in cold seasons (Fig.1(b)/(e)). H_2SO_4 concentration exceeds 10^7 cm^{-3} only on a few days in Beijing, whereas it is a common phenomenon in Nanjing daytime. Besides H_2SO_4 , we report the first long-term measurement of HIO_x in urban environments continued from earlier sparse measurements (He et al., 2021b). The calibrated HIO_x concentration is above the detection limit during almost the entire measurement periods, indicating a clear presence of HIO_x in inland cities. The HIO_3 concentration was between 10^5 and 10^6 cm^{-3} for most of the time except for winter months; it sporadically approaches or is higher than 10^6 cm^{-3} in warm months. On the other hand, iodous acid, HIO_2 is less abundant than HIO_3 at both sites with a general concentration at around 10^4 cm^{-3} and a maximum concentration approaching 10^5 cm^{-3} in the summer. The results indicate that the H_2SO_4 concentrations are generally higher than that of iodine oxoacids at both sites. As for the two iodine oxoacids (HIO_3 and HIO_2), daytime mean concentration of HIO_3 is more than one order of magnitude higher than HIO_2 . The



one order of magnitude lower HIO_3 concentration compared with H_2SO_4 in summer at both sites is consistent with that in the Finnish subarctic boreal forest (Jokinen et al., 2022).

315 The frequencies of NPF events varied significantly, from none to more than three quarters of the days in each month during the measurement period. The occurrence of NPF events in China is favoured by various meteorological factors (Qi et al., 2015; Zhou et al., 2021; Chu et al., 2019). However, the influences can be quite uncertain and complex because of different season and the location of measurement site. Take temperature for an example, on one hand, warm temperatures enhance the

320 abundance of biogenic and anthropogenic volatile organic compound emissions as well as their oxidation processes (Paasonen et al., 2013; Paasonen et al., 2018; Nie et al., 2022; Ehn et al., 2014). On the other hand, the warm temperature also reduces the stability of embryonic clusters thus reducing nucleation and subsequent growth rates (Kürten et al., 2016). Besides meteorological conditions, vapour condensation sink (CS) and particle coagulation sink (CoagS) have negative effects on the NPF frequency

325 (Kalkavouras et al., 2017; Bousiotis et al., 2021; Wehner et al., 2007). Decreased CS and/or CoagS will lead to faster nucleation and subsequent growth (as scavenging of nucleating and condensable vapours is less effective) and higher survival probability through the growth processes during NPF events (as the scavenging of clusters and small particles is less effective). As expected, the concentration of gaseous H_2SO_4 is notably correlated with NPF frequency, as H_2SO_4 is the most important compound to form

330 initial clusters and one of the main contributors to the growth of newly formed particles (Nieminen et al., 2010; Kirkby et al., 2011). During this measurement, the ratio of $\text{GR}_{1.5-3}$ contributed from H_2SO_4 to measured GR calculated from MOD is about 72.4% (shown in Table S4).

As depicted in Figure 1(c)/(f), the frequencies of NPF for each month at two sites are quite different,

335 since environments are chemically complex and diverse with many aforementioned factors influencing NPF. Generally, NPF events are more likely to occur in the spring and winter, with the lowest frequency in summer at BUCT station in Beijing, consistent with other reports (Wu et al., 2007; Deng et al., 2020b). Different from Beijing, there are less NPF events in the winter than in the summer at SORPES station, which is in line with a long-term measurement conducted at the same site (Qi et al., 2015). It could be

340 attributed to the lowest H_2SO_4 concentration in cold season, which was found to be the main driver for NPF events in polluted megacities in China (Yao et al., 2018). Another explanation may be that the high CS in the winter daytime (Qi et al., 2015) suppresses the NPF events. It should be noted that the particle



formation mechanism in Nanjing is yet to be revealed and NPF intensity could be reduced if DMA is limited in Nanjing.

345 3.2 Characteristic of acid concentrations

3.2.1 Seasonal variation

To better understand the roles of the studied acids in new particle formation and growth, we further present the seasonal variation of H_2SO_4 , HIO_3 and HIO_2 concentrations in Fig. S3. It depicts the monthly statistics of H_2SO_4 and HIO_x at the two sites with different shadings indicating seasons. Both H_2SO_4 and HIO_x concentrations in Nanjing are always higher than those in Beijing except for H_2SO_4 concentrations in the winter. We speculate that the generally higher acid concentrations in Nanjing are caused by stronger solar radiation at latitude of $32^\circ 07' \text{N}$ in Nanjing, compared with $39^\circ 56' \text{N}$ in Beijing. On the other hand, the reason of higher wintertime H_2SO_4 concentrations in Beijing is likely due to the higher SO_2 and more frequent sunny weather during the winter in Beijing (Wang et al., 2018) and further discussion can be seen in supplementary materials. At both sites, the seasonal pattern of H_2SO_4 is not very strong (Deng et al., 2020b; Petäjä et al., 2009). H_2SO_4 concentrations are higher in the spring and autumn, lower in the summer, and lowest in the winter.

The HIO_3 concentrations measured at the two sites are significantly lower than that at pristine coastal site (e.g., in Mace Head (Sipilä et al., 2016)). Measurements at Mace Head indicate that HIO_3 concentrations are frequently above 10^7 cm^{-3} with some days exceeding 10^8 cm^{-3} in September. The concentrations of atmospheric iodine at coastal sites are normally higher due to active biogenic emissions of iodine-containing precursors from marine algae (O'dowd et al., 2002). On the other hand, HIO_3 concentrations in Beijing and Nanjing are comparable to that in Helsinki, Finland. Measurements at SMEAR III station, an urban site located in University of Helsinki show HIO_3 concentrations at around 10^6 cm^{-3} when the wind is coming from land for most times in August and HIO_3 concentrations exceed 10^7 cm^{-3} when air masses have marine origin (Thakur et al., 2022; He et al., 2021b). Another long-term observation conducted at SMEAR I station (Jokinen et al., 2022), a subarctic boreal forest site, shows HIO_3 concentrations often at around 10^5 cm^{-3} from April to November 2019 (summer and autumn) with occasional peaks exceeding 10^6 cm^{-3} in late August. HIO_x concentrations at AHL/BUCT station depict a distinctly unimodal pattern in a year cycle with highest values in July, increasing from January and decreasing to December. However, seasonal variations of HIO_x are slightly different at SORPES, as there



are similar levels of HIO_x throughout the summer in 2019, reaching a seemingly steady daily maximum. HIO_3 concentration measured from August to September in 2018 over the central Arctic Ocean increases significantly from summer towards autumn (Baccarini et al., 2020), which is different from the results in
375 both Beijing and Nanjing, due to significantly different environments and iodine sources.

3.2.2 Diurnal pattern

Though the HIO_3 concentrations are different in four seasons, the diurnal patterns are similar throughout the year (Fig. 2). Daily trends of both median H_2SO_4 and HIO_x concentration are strongly connected with
380 diurnal cycle. The concentration of HIO_x increases at the same time as H_2SO_4 , i.e., both HIO_x and H_2SO_4 rise in the early morning and peak from noon to afternoon. The clear diurnal pattern of H_2SO_4 has been attributed to photochemical activities (Lu et al., 2019; Yang et al., 2021; Petäjä et al., 2009). Hydroxyl radical (OH) is the most important oxidant for sulfur dioxide (SO_2) to form daytime H_2SO_4 (Guo et al., 2021; Yang et al., 2021). Therefore, the diurnal pattern of H_2SO_4 would be affected by its precursors (e.g.,
385 SO_2 and OH in daytime). Higher HIO_x concentrations in the daytime and the absence of their nocturnal maxima suggest that the main source of HIO_x is also photochemical oxidation of iodine precursor vapours. The distinct diurnal variation in HIO_x concentration with around one order of magnitude implies fast in-situ chemistry. Although the diurnal patterns of H_2SO_4 and HIO_3 are alike, the occurrence of HIO_3 daytime maximum is on average later than that of H_2SO_4 at both sites (Fig. 2). This phenomenon is
390 pronounced during summer daytime when daily maximum of H_2SO_4 appears around 2 hours earlier than that of HIO_3 . It implies that albeit these two acids form during daytime through photochemical pathways, the limiting factors for their productions can be different. At the SORPES station, for instance, the diurnal cycle of H_2SO_4 follow that of radiation in spring, summer and winter. In summer, however, owing to effectiveness of long-term emission reduction, SO_2 concentrations can be low enough to limit the
395 production of H_2SO_4 (Ding et al., 2019), so the daytime peaks of H_2SO_4 tend to occur when SO_2 reached its daily maximum (Yang et al., 2021). On the other hand, little is known about the diurnal patterns of HIO_x in urban environments. It was demonstrated in chamber experiments that HIO_x can be formed by oxidation of oxidised iodine species with ozone in the absence of HO_x (He et al., 2021b) and $\text{I}_2\text{O}_2 + \text{O}_3$ reaction was recently found to be the critical step for the HIO_3 formation (Finkenzeller et al., 2023). The
400 authors found that ambient level of O_3 was not the limiting factor for HIO_3 formation. However, the



maximum of HIO_3 was found to mimic that of O_3 , indicating that O_3 may influence terrestrial HIO_3 formation. One such possibility is that the source of iodine is controlled by O_3 deposition, e.g., a similar process to that occurring over marine surfaces (Carpenter et al., 2013). This mechanism mainly explains the inorganic iodine emissions from marine environments, but a similar process may also occur in
405 polluted urban environments although the iodine source in urban environments is yet to be discovered. Another possibility is that air temperature may strongly perturb the formation of HIO_3 and the release of iodine precursors, which will be discussed in detail in the next section.

Moreover, CS in Nanjing shows an opposite profile to T and O_3 , whereas it keeps almost the same trend
410 as that of Nanjing but fluctuates a little during the day in Beijing spring and winter, which show median values only in 2019. In summary, the diurnal patterns shown in Fig. 2 suggest that stronger solar radiation coupled with higher mixing ratio of O_3 and higher T are likely the factors favouring the formation of acids, the low CS at noon is preferred for the survival of acid vapour. Additionally, the diurnal variation of HIO_x at BUCT shows stronger seasonality with highest values at around noon in the summer. The
415 maximum concentrations at spring and autumn are similar, while the maximum concentrations in the winter are roughly one order of magnitude lower. At SORPES, HIO_x reaches similar levels in the spring, summer and autumn but its concentration is lower in the winter. Consistently, the diurnal maximum HIO_3 concentration in summer approaches 10^6 cm^{-3} at both sites.

420 3.2.3 Iodine sources

In order to investigate the source of HIO_x in urban environments, we further conduct cluster analysis of the air mass backward trajectories of the AHL/BUCT station. The HIO_3 precursor proxy calculated from Eq. (13) based on the measurement results at BUCT/AHL station is classified into four levels as shown in Fig. S4. High precursor levels are mainly associated with air masses originating from the south and
425 southeast, whereas lower iodine precursor concentrations are associated with northern air masses. It implies that marine iodine sources could be important for the AHL/BUCT station due to long range transport. Additionally, higher concentration of iodine precursor when the air mass travels from southern land indicates that the continental outflows may also play a significant role in transporting HIO_3 precursors. Therefore, both marine (O'dowd and Hoffmann, 2005; Carpenter et al., 2021) and terrestrial



430 precursors (Li et al., 2014; Wang et al., 2017) may contribute to the HIO₃ formation at the AHL/BUCT site.

Both seasonal variation and diurnal pattern shows the lowest concentration of HIO_x in winter when the impact from residential coal burning and fossil fuel combustion power plant in Beijing is the largest. It implies that HIO_x concentration is not promoted by pollution in cold season. A previous 2-year measurements conducted in Beijing show that high loadings of particulate organic iodine compounds (OICs) occurred in the heating season, and HOI was thought to be the key oxidant to form the OICs (Shi et al., 2021). The different seasonal distribution between gaseous HIO_x in this study and particle-phase OICs indicates potentially different iodine sources of gaseous and particulate phases, which warrants further investigation. Figure 3a presents HIO₃ in different PM_{2.5} ranges and shows lower HIO₃ concentrations when PM_{2.5} increases. PM_{2.5} measurements in the Beijing–Tianjin–Hebei region (2013 to 2020) show obvious seasonal characteristics with lowest concentrations in summer and highest concentrations in winter (Yang et al., 2022). This phenomenon should be attributed to the inherently independent seasonality of these two constituents instead of any correlation. If the PM_{2.5} is a source of gaseous iodine species, the HIO₃ concentrations should be higher in winter months, which is not the case. Additionally, summertime HIO₃ concentrations in different PM_{2.5} concentration bins have no difference (Fig. 3b), which further indicates that the HIO₃ is not correlated with the particulate matter pollution in Beijing.

450 There is no definite evidence to justify whether marine or land sources could better explain our observation on HIO₃ concentration in Beijing. In the marine environments, the rapid reaction of sea-surface iodide with O₃ is believed to be the largest global source of iodine species in the forms of molecular iodine, I₂ and hypoiodous acid, HOI (Carpenter et al., 2021; Carpenter et al., 2013), which in turn contributes to the formation of HIO_x (Finkenzeller et al., 2023; He et al., 2021b). However, the photolysis lifetimes of HOI (~140 s) and I₂ (~10 s), or biogenic volatile iodocarbons (e.g., CH₂I₂ (~5 min)) are too short to contribute to the formation of HIO_x in Beijing and Nanjing considering the long-range transportation (Saiz-Lopez et al., 2012). Another iodine-containing species, methyl iodide (CH₃I), has a longer lifetime of about 5 days which may potentially go through the long-range transportation and eventually reach inland cities. CH₃I is dominantly formed from photochemical processes in the marine



460 surface (Moore and Zafiriou, 1994) and additionally also from dust stimulated abiotic emission (Williams
et al., 2007). CH₃I concentration was shown to be correlated with surface seawater temperature (SST) in
marine boundary layer air at midlatitude (Yokouchi et al., 2008). Others reported the opposite results in
the Yellow Sea and the East China Sea during summer (Li et al., 2021) and the reason may be that higher
surface water temperature also accelerates the chemical loss of CH₃I from the seawater and atmospheric
465 CH₃I is readily photolyzed. Long-term variations of atmospheric CH₃I at several sites show that SST
near each site cannot fully explain the variation of observed CH₃I concentrations (Yokouchi et al., 2012).
Other factors such as acidification, i.e., pH conditions, mineral dust deposition and dissolved organic
carbon (DOC) concentration (Li et al., 2021), as well as ferric ion (Fe³⁺) concentration (Chen et al., 2020)
in seawater could also contribute to the emission rate of CH₃I.

470

Apart from marine sources, terrestrial sources of CH₃I including most rice paddies (Redeker et al., 2000),
terrestrial biomes (Sive et al., 2007), and minor wetlands (Dimmer et al., 2001), biomass burning
(Andreae et al., 1996) were also proposed. High concentration of CH₃I at two inland sites in Japan
indicates the greater importance of terrestrial sources in the summer compared to oceanic sources
475 (Yokouchi et al., 2008). As CH₃I emission from rice paddies is positively correlated with temperature
(Redeker and Cicerone, 2004; Redeker et al., 2000), CH₃I emission is likely to be stronger in the
summertime. This is consistent with higher concentrations of HIO_x in Beijing and Nanjing as shown in
Fig. 1, 2 and 4. Moreover, experiments show that CH₃I emission under dark incubation was much lower
than that under light incubation and CH₃I production under visible light conditions is lower than that
480 under natural light (Li et al., 2021). Those results indicate that ultraviolet light promotes the production
of CH₃I (Chen et al., 2020; Li et al., 2021) as well as its photochemical oxidation. This is consistent with
our observation that HIO_x is only formed in the daytime (Fig. 4).

The relative importance of terrestrial and marine iodine sources may vary widely with local
485 meteorological factors and the transportation of air masses. Future efforts are needed to verify the
composition and distribution of HIO_x precursors in polluted environments.



3.2.4 Formation of HIO₃ in urban environments

Quantum chemical methods and laboratory experiments have both been carried out to investigate the formation mechanisms of HIO₃. Previous studies using quantum chemical calculations have proposed two possible formation pathways of HIO₃. Iodine monoxide (IO) was proposed to react with HO₂ radical to yield HIO₃ (Drougas and Kosmas, 2005). The reaction between iodine dioxide (OIO) and OH radical was also suggested to produce HIO₃ (Plane et al., 2006). Laminar flow reactor experiments have also been carried out to investigate the formation mechanisms of HIO₃ from I₂ (He, 2017). With the illumination of green-fluorescent lamp, I₂ was efficiently photolyzed while O₃ photolysis was restricted, and thus there was no known source of HO_x. Surprisingly, a significant amount of HIO₃ was formed essentially under HO_x free conditions. To rule out a potential unknown OH source in the flow reactor, different OH scavengers (methane, sulfur dioxide, cyclohexene and acetic acid) were injected but the production of HIO₃ remained. Iodine atoms or iodine oxides were proposed to be the reactants with ozone and water to produce HIO₃. Following studies from the CLOUD experiments suggest that iodoxy hypiodite (IOIO) could be efficiently converted into HIO₃ via reactions R (1) and R (2) (Finkenzeller et al., 2023) which successfully explain earlier laboratory and field observations (Sipilä et al., 2016; He et al., 2021b). These results align with our observations at the AHL/BUCT station. UVB is an indication of light intensity and influences the production of I atoms from the photolysis of I₂ and CH₃I. The produced iodine atoms react with O₃ and further drive gaseous iodine chemistry (Saiz-Lopez et al., 2012). Fig. 4 depicts the correlation of UVB, O₃ and temperature. Although the correlation between HIO₃ concentration and air temperature is not very strong, high HIO₃ concentrations appear when both the UVB and O₃ mixing ratios are high. This is consistent with the fact that both solar radiation and O₃ are required to initiate the iodine emission and iodine photochemistry.

510



3.3 Iodic acid enhances the particle survival probability

515 Statistical results show that NPF events occur frequently at both sites throughout the measurement periods. Whether freshly nucleated particles can contribute to cloud condensation nuclei and hence



impose influence on climate and human health depends largely on how fast they grow into larger particles and survive from coagulation scavenging by pre-existing aerosols, which is more efficient for smaller particles. The GR of newly formed particles is therefore central for sub-10 nm particle lifetimes in ambient environment. Earlier studies have linked some dimensionless parameters L or L_r (McMurry et al., 2005; Kuang et al., 2010; Cai et al., 2017b) to justify the occurrence of NPF and described the competition between aerosol surface area and condensable vapours during the growth period. Recently, a dimensionless survival parameter P (Kulmala et al., 2017) was proposed as the ratio of CS' ($CS/10^{-4} s^{-1}$) to GR' ($GR/1nm\ hour^{-1}$). From this ratio, P shows the competition between the possibility of being cleared and growing to survive. When P is below 50 in clean environment or 100 in polluted urban cities, the SP of the sub-3 nm particles is agreed with the atmospheric observations. As shown in Fig. S6, the median P is about 50 for the sub-3 nm particles, whereas the median P value is about 20 for 3-7 nm particles in the NPF events at the AHL/BUCT station. That means the growing particles in those days preferred to survive and thus showed us clear new particle formation and further growth.

530

As shown in Eq. (8), the impact of GR on survival of new particles is not linear and a small enhancement on GR could result in much larger enhancement in particle survival probability. To further illustrate the non-linear response of particle SP, we plot the logarithmic value of SP ($\log_{10} SP$) as a function of CoagS and GR from 1.5 to 3 nm (Fig. 5 panel a) and from 3 to 7 nm (Fig. 5 panel b), respectively. The value of SP is extremely sensitive both to CoagS and GR. Under the typical CoagS (around $0.0025 s^{-1}$) at both sites, the SP could be enhanced by more than two orders of magnitude when GR is varied from 1 to 10 $nm\ h^{-1}$. Increased GR caused by additional condensing vapours enables faster growth, which in turn facilitates the survival of sub-10 nm particles from coagulation scavenging. This effect is especially important for sub-3 nm particles as they are the most susceptible and are easily lost to large pre-existing particles. A limited variation of GR was suggested to cause considerable variation of SP (Cai et al., 2021a).

540

We present case studies of several consecutive NPF events at both sites in Fig. 6. At AHL/BUCT station, NPF events occurred from May 25 to 29, 2021 due to favourable meteorological conditions, except for one undefined day (May 27, 2021) when no obvious growth was observed. On this undefined day, the UVB in the daytime was low and the intensity was fluctuating, due to cloudiness. Both of these

545



conditions, as well as the higher CS, suppressed the NPF (Kerminen et al., 2018; Deng et al., 2020a; Cai et al., 2021b). On the other hand, both T and O₃, as well as UVB, increased from around 6:00 in the morning on the NPF event days, with decreasing RH. The averaged concentrations of H₂SO₄ and HIO₃ in the particle growth periods from 1.5 nm to 7 nm on event days and from 8:00 to 10:00 on the other days were summarized in Table 1. The ratio of HIO₃ concentration to H₂SO₄ was about 5% in the first three days and more than 10% in the next two days, likely due to higher O₃ concentrations which contributes to the emission of iodine precursors.

Table S2–S4 and S5–S7 summarise the HIO₃ contribution to GR and SP in the particle size range of 1.5–3 nm and 3–7 nm, respectively. To account for the uncertainties in the GR and SP calculations, the measured GR are calculated using three methods, namely the APT-*x*, APT-*y* and the mode-fitting (MOD) methods (see Methods part, Fig. S7). We present the results from MOD methods in the main text to keep consistency with earlier studies (Deng et al., 2020b; Qiao et al., 2021). Only events with clear growth were reported in this study to reduce systematic uncertainties resulting from the GR calculation. We also provide the results from the APT-*x* and APT-*y* methods in the supplementary materials for completeness. The results in Table S2-S4 show that the contributions of HIO₃ to GR_{<3} on May 25 and 26 were lower than 5%, whereas the contribution was more than 10% on May 29. The SP_{1.5-3} enhancement from HIO₃ is much stronger on May 29, even reaching 40.5%. Although the contribution of HIO₃ to GR_{<3} on Jun 21, 2021 is almost identical to that on May 29, 2021, SP enhancements on Jun 21, 2021 is 2.5 times larger. This is a result from the 5 times CoagS on Jun 21, 2021. This suggests that in polluted environments with higher CoagS, such as Beijing, a fixed GR enhancement can lead to larger SP enhancements. Results in both Fig. 7 and Fig. S5 show that the median contribution of HIO₃ to the GR of particles in the 1.5–3 nm size range is 7.4% using the MOD method, whereas the contribution is only around 3% and 2% using the APT-*x* and APT-*y* methods, respectively. This is resulted from the difference in the measured GR calculated using either the APT or the MOD methods. This further translates into 10.8%, 4.1%, 40.5% SP EF using MOD, APT-*x* and APT-*y* methods, respectively. Despite the uncertainty in the measurement GR calculation, the EF of HIO₃ to sub-3 nm particle SP is clear: in 33.3%, 25.0% and 55.6% of the events HIO₃ enhances particle SP by more than 30%, using MOD, APT-*x* and APT-*y* methods, respectively.



580 Additionally, we show three consecutive NPF events observed from 16 to 18 August 2019 at the SORPES station, Nanjing. These events feature high acid concentrations, O₃ mixing ratios and strong light intensities as well as low RH and CS. No nucleation mode particles burst was observed on August 20 probably owing to decreased H₂SO₄ concentration. Compared to the cases in Beijing, the concentrations of O₃ and acids are twice as higher at the SORPES station due to geographical and seasonal differences (Table 1).

585 From June to December 2019, there are 23 NPF events recognized at the SORPES station. Due to the detection limitation of the instruments at SORPES, the sub-3 nm particles were not clearly measured, which in turn poses challenges to get the measured GR through the 50% appearance time method nor the mode fitting method. The statistics are depicted in a different way from that of the AHL/BUCT (see supplementary materials for further details). Briefly, the contribution of HIO₃ and H₂SO₄ to sub-3 nm particle GR in NPF events are quantified based on Eq. (9), Eq.(10) and Eq.(11). This is based on the observed consistency between the gaseous H₂SO₄ concentration and its significant contribution to the sub-3 nm particle growth rate in Beijing (Deng et al., 2020b). The SP enhancement is further calculated 590 based on Eq. (12). Consistent with the observation at the AHL/BUCT station, the concentration of gaseous HIO₃ in Nanjing is lower than H₂SO₄ throughout the measurement period, accounting for 10~20% of concentration (Fig. 1e). However, the average HIO₃:H₂SO₄ ratio (16.8%) is higher than that in Beijing (10.7%).

595 The calculated GR contribution of IA and SA to sub-3 nm particles (Ratio_{1.5-3}) are listed in Table S8, respectively, where the statistical ratios of acid contributions for each NPF event are listed as well. The computations of Eq. (9) and Eq. (10) are subject to acid concentrations and hence the average acid concentrations for individual NPF events dominate the statistics of GR ratio. At the SORPES station from June to November 2019, HIO₃ contributes 6.1% (median) and 6.7% (mean) to sub-3 nm particles growth compared to H₂SO₄.

600

As listed in Table S9, estimated particle survival probability of particles growing from 1.5 to 3 nm considering H₂SO₄ as the governing contributor (SP_{1.5-3}(SA)) is significantly enhanced when counting the contribution from HIO₃ (SP_{1.5-3}(SA+IA)). The enhancement of SP with IA being an additional GR contributor varies from 3% to more than 100% in favourable cases, with a median enhancement of 54.3%. 605 For sub-3 nm particles, the survival probability is twice as higher (enhancement factors exceeding 100%)



considering HIO_3 as additional GR contributor on July 3 and October 26. As depicted in Fig. S8(c), SP enhancements in percentage are generally one order of magnitude higher than the GR contribution in percentage and HIO_3 can result in as high as 2-fold enhancement on SP in sub-3 nm particle growth.

610 The statistical results at both sites suggest that for polluted environments with higher CoagS, GR enhancement is especially important for the survival of small particles. In Beijing, HIO_3 contributes 7.4% (median) to sub-3 nm particle growth and 2.6% (median) to 3-7 nm particle growth in all NPF events from May to September. Despite the limited GR contribution, it could lead to 40.5% enhancement of $\text{SP}_{<3}$, whereas there is only a negligible increase of 3.2% (median) for SP_{3-7} , estimated using the
615 MOD method. In exceptional cases, we found that HIO_3 could enhance particle SP by more than two-fold in 22.2% of cases. The median value of GR contribution of HIO_3 accounts for 6.1% of H_2SO_4 and the median enhancement of 1.5-3 nm particles survival probability reaches 47.6% when consider HIO_3 as an additional GR contributor, at the SORPES station in summer 2019. In favourable cases, the gaseous HIO_3 can contribute to more than 14.0% of particle growth, leading to the survival probability of fresh
620 particles enhanced by a factor of two. The role of the other iodine oxoacid, HIO_2 , in particle growth remains unclear due to the absence of contribution equation like Eq. (10) for HIO_3 . The estimated contribution of HIO_2 derived from the same equation should be significantly smaller compared with that of HIO_3 even if the arrival rate of HIO_2 also reaches the kinetic limit, as measured HIO_2 concentrations at both sites are much lower than HIO_3 .

625 In summary, our findings show that HIO_3 is an important contributor to sub-3 nm particle survival in these two Chinese cities and similar environments elsewhere in warm seasons. However, for particles in 3-7 nm, the contribution of HIO_3 to particle GR and SP is negligible.

4 Conclusion

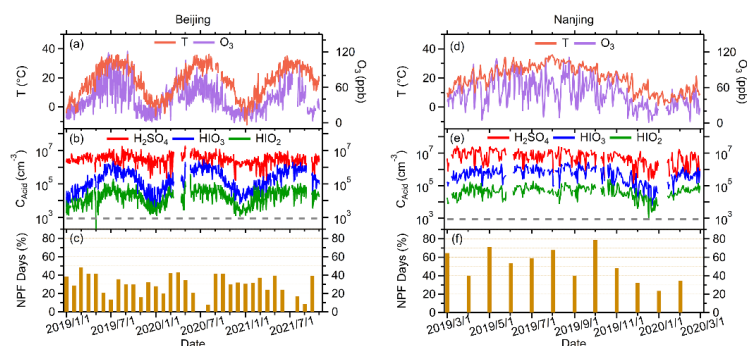
In this study, we show three years' measurements of iodine oxoacids (HIO_x) in Beijing and one-year
630 observation in Nanjing. Unlike H_2SO_4 , HIO_3 has a more prominent seasonal variation at both sites with highest concentrations in summer and lowest concentrations in winter. The diurnal pattern of HIO_x indicates that HIO_3 formation is influenced by photochemical activities and O_3 concentrations which may together influence the emission of iodine species and the further oxidation chemistry. In Beijing, back



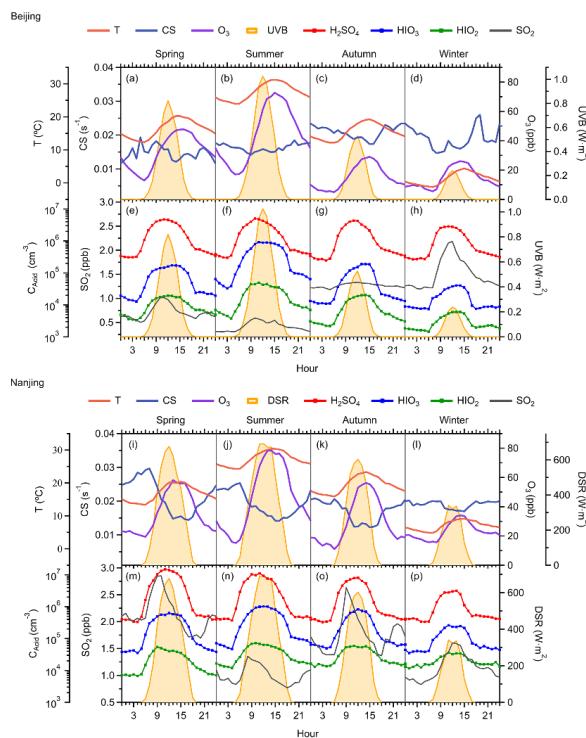
trajectory analysis suggests that marine iodine sources are important for the HIO_x production and less
635 HIO_x is observed if the air masses originate from the North. The lowest concentrations of HIO_x in winter
and its weak correlation with $\text{PM}_{2.5}$ implies that anthropogenic activities are likely not the important
sources of HIO_x .

We find that the median contribution of iodic acid, HIO_3 , to $\text{GR}_{\text{sub-3}}$ is less than 10% in Beijing and in
640 Nanjing from May to September. However, HIO_3 can significantly enhance particle survival probability,
occasionally by two-fold, for 1.5-3 nm particles at both sites. This means that although H_2SO_4 is
considered to be the main driver of sub-3 nm growth in polluted urban areas, additional sources, such as
 HIO_3 , needs to be considered. As the growth rate of HIO_3 is measured to be identical to that of H_2SO_4 on
a per-molecule basis (He et al., 2021b), we propose that HIO_3 and H_2SO_4 can be summed up when
645 estimating the sub-3 nm particle growth rates. Beside the enhancement on particle growth, recent
theoretical studies have indicated that dimethyl amine could potentially accelerate pure HIO_3 nucleation
(Ning et al., 2022). However, experimental confirmation is needed to confirm such prediction and our
long-term observation can therefore provide basis for guiding experimental works to use ambient relevant
level acid concentrations.

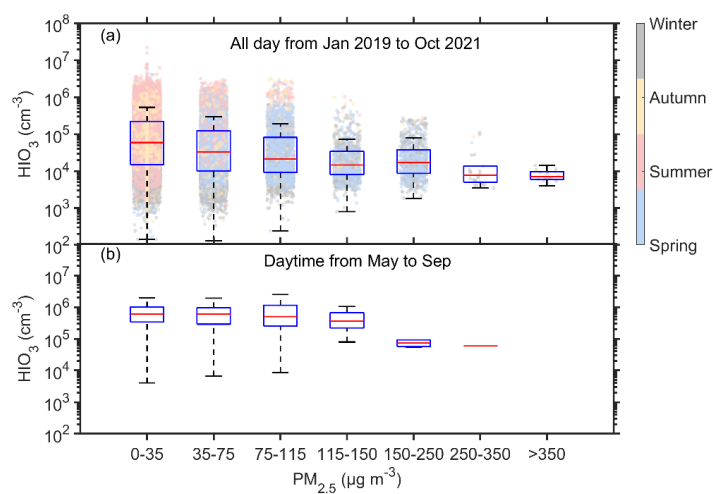
650



655 **Figure 1.** Timeseries of parameters from Jan 1, 2019 to Oct 31, 2021 in Beijing (a-c) and from March 1, 2019 to Feb 29, 2020 in Nanjing (d-f). (a/d). Temperature and ozone; (b/e). Sulfuric acid and iodine oxoacid concentrations. The grey dashed line represents the detection limit of instruments (875 cm^{-3}); (c/f). The frequencies of new particle formation events in each month. Time resolution for all the presented data is 1 day and the environmental parameters and vapour concentrations are averaged daytime (8 am to 4 pm) mean.



660 **Figure 2.** Diurnal variation of median value of O_3 , T, and CS in the first row (Beijing, a-d) and third row (Nanjing, i-j) and the diurnal variation of median SO_2 , H_2SO_4 and HIO_x concentrations in the second row (Beijing, e-h) and fourth row (Nanjing, m-p) in four seasons. The first to last columns are profiles in spring, summer, autumn, and winter, respectively. The diurnal patterns of UVB were plotted in every panel to compare with other factors better.



665 **Figure 3.** HIO₃ concentration in different PM_{2.5} level bins. (a) data from the whole campaign coloured by the seasons in Beijing and (b) data in the daytime from May to September (warm seasons) in Beijing.

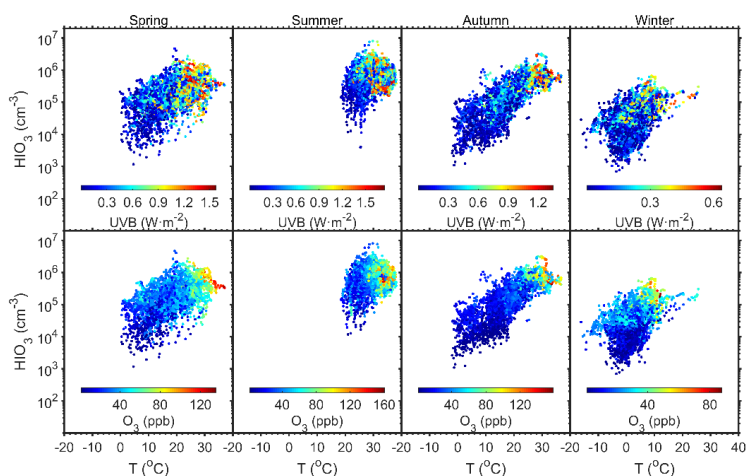
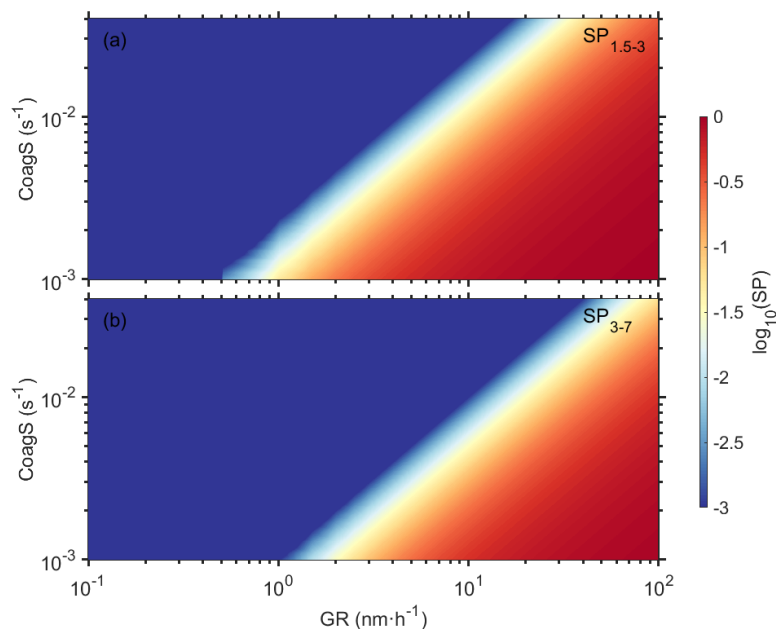
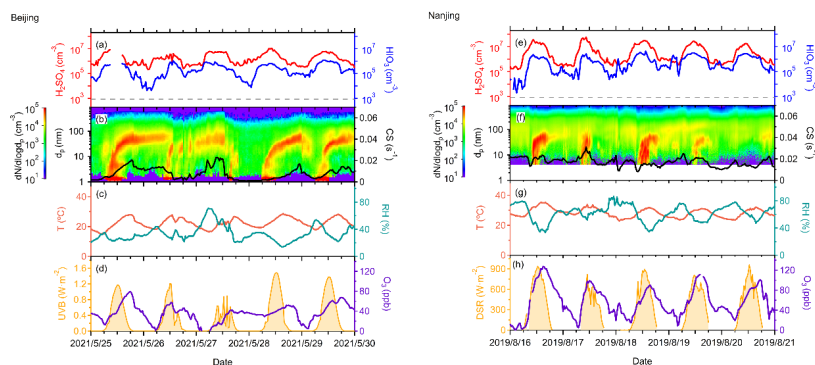


Figure 4. Influences of T, UVB, and O₃ on HIO₃ concentration in the daytime (8:00-16:00) in Beijing. The analysis is separated into four seasons.



670 **Figure 5.** The effect of coagulation sink and growth rate on particle survival probability for 1.5-3 nm (a) and
 3-7 nm (b) particles, respectively.



675 **Figure 6.** Cases of consecutive NPF events in Beijing (a-d) and Nanjing (e-h) sites. Acid concentrations are
 shown in the first row, particle number size distribution, and CS are shown in the second row, meteorological
 factors, such as T, RH, UVB, and O₃ concentrations are also presented in the third and fourth rows. The
 measurement of acids in the Beijing site was unavailable for a short period on May 25 (panel (a)).

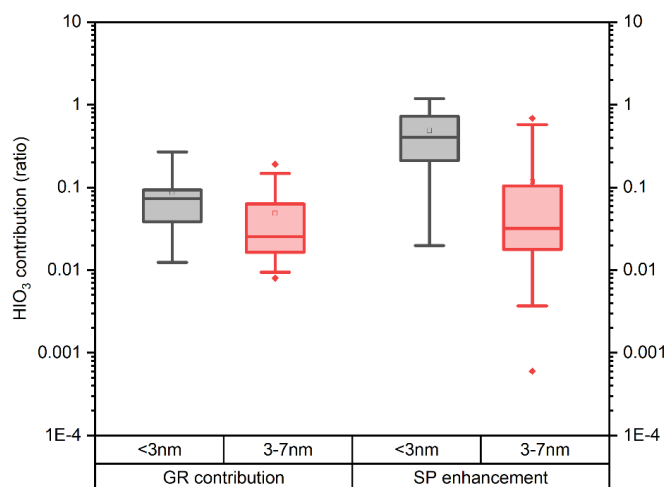


Figure 7. The contributions in ratio of HIO_3 to growth rate (a) and survival probability enhancement (b) of particles within sub-3nm and 3-7nm in NPF events in the Beijing site utilizing the mode fitting method.

680

Table 1. Environmental factors and acid concentrations shown in Figure 5.

Site	Date	Start time	End time	H_2SO_4 (cm^{-3})	HIO_3 (cm^{-3})	CS (s^{-1})	T ($^\circ\text{C}$)	RH (%)	UVB/DSR (W/m^2)	O_3 (ppb)
Beijing	2021/5/25	6:50:00	9:23:00	3.96E+06	2.03E+05	0.0046	18.5	26	0.20	25.68
	2021/5/26	9:20:00	10:48:36	8.01E+06	4.90E+05	0.0105	24.25	32	0.84	47.82
	2021/5/27	8:00:00	10:00:00	1.66E+06	5.41E+04	0.0222	19.6	59	0.45	11.17
	2021/5/28	6:00:00	8:15:00	5.35E+06	7.21E+05	0.0018	20.35	34	0.10	31.51
	2021/5/29	6:20:00	9:38:44	3.89E+06	4.99E+05	0.0040	19.4	50	0.25	31.24
Nanjing	2019/8/16	10:22:21	14:59:49	2.03E+07	1.40E+06	0.0200	33.23	40.69	858	105.38
	2019/8/17	8:04:22	11:10:40	4.27E+07	1.79E+06	0.0268	32.02	56.43	525	75.27
	2019/8/18	10:17:53	17:18:42	2.06E+07	2.20E+06	0.0134	30.93	39.52	705.1	81.09
	2019/8/19	8:00:00	10:00:00	1.35E+07	2.48E+06	0.0164	27.99	61.71	419.7	58.72
	2019/8/20	8:00:00	10:00:00	1.07E+07	2.12E+06	0.0154	27.4	67.08	458	48.26



Reference:

- 685 Almeida, J., Schobesberger, S., Kürten, A., Ortega, I. K., Kupiainen-Määttä, O., Praplan, A. P., Adamov, A., Amorim, A., Bianchi, F., Breitenlechner, M., David, A., Dommen, J., Donahue, N. M., Downard, A., Dunne, E., Duplissy, J., Ehrhart, S., Flagan, R. C., Franchin, A., Guida, R., Hakala, J., Hansel, A., Heinritzi, M., Henschel, H., Jokinen, T., Junninen, H., Kajos, M., Kangasluoma, J., Keskinen, H., Kupc, A., Kurtén, T., Kvashin, A. N., Laaksonen, A., Lehtipalo, K., Leiminger, M., Leppä, J., Loukonen, V.,
- 690 Makhmutov, V., Mathot, S., McGrath, M. J., Nieminen, T., Olenius, T., Onnela, A., Petäjä, T., Riccobono, F., Riipinen, I., Rissanen, M., Rondo, L., Ruuskanen, T., Santos, F. D., Sarnela, N., Schallhart, S., Schnitzhofer, R., Seinfeld, J. H., Simon, M., Sipilä, M., Stozhkov, Y., Stratmann, F., Tomé, A., Tröstl, J., Tsagkogeorgas, G., Vaattovaara, P., Viisanen, Y., Virtanen, A., Vrtala, A., Wagner, P. E., Weingartner, E., Wex, H., Williamson, C., Wimmer, D., Ye, P., Yli-Juuti, T., Carslaw, K. S.,
- 695 Kulmala, M., Curtius, J., Baltensperger, U., Worsnop, D. R., Vehkamäki, H., and Kirkby, J.: Molecular understanding of sulphuric acid–amine particle nucleation in the atmosphere, *Nature*, 502, 359–363, 10.1038/nature12663, 2013.
- Andreae, M. O., Atlas, E., Harris, G. W., Helas, G., de Kock, A., Koppmann, R., Maenhaut, W., Manó, S., Pollock, W. H., Rudolph, J., Scharffe, D., Schebeske, G., and Welling, M.: Methyl halide emissions
- 700 from savanna fires in southern Africa, *Journal of Geophysical Research: Atmospheres*, 101, 23603–23613, 10.1029/95jd01733, 1996.
- Baccarini, A., Karlsson, L., Dommen, J., Duplessis, P., Vullers, J., Brooks, I. M., Saiz-Lopez, A., Salter, M., Tjernstrom, M., Baltensperger, U., Zieger, P., and Schmale, J.: Frequent new particle formation over the high Arctic pack ice by enhanced iodine emissions, *Nature Communications*, 11, 4924,
- 705 10.1038/s41467-020-18551-0, 2020.
- Beck, L. J., Sarnela, N., Junninen, H., Hoppe, C. J. M., Garmash, O., Bianchi, F., Riva, M., Rose, C., Peräkylä, O., Wimmer, D., Kausiala, O., Jokinen, T., Ahonen, L., Mikkilä, J., Hakala, J., He, X. C., Kontkanen, J., Wolf, K. K. E., Cappelletti, D., Mazzola, M., Traversi, R., Petroselli, C., Viola, A. P., Vitale, V., Lange, R., Massling, A., Nøjgaard, J. K., Krejci, R., Karlsson, L., Zieger, P., Jang, S., Lee, K., Vakkari, V., Lampilahti, J., Thakur, R. C., Leino, K., Kangasluoma, J., Duplissy, E. M., Siivola, E.,
- 710 Marbouti, M., Tham, Y. J., Saiz-Lopez, A., Petäjä, T., Ehn, M., Worsnop, D. R., Skov, H., Kulmala, M., Kerminen, V. M., and Sipilä, M.: Differing Mechanisms of New Particle Formation at Two Arctic Sites, *GRL*, 48, 10.1029/2020gl091334, 2021.
- Bousiotis, D., Brean, J., Pope, F. D., Dall'Osto, M., Querol, X., Alastuey, A., Perez, N., Petäjä, T., Massling, A., Nøjgaard, J. K., Nordström, C., Kouvarakis, G., Vratolis, S., Eleftheriadis, K., Niemi, J. V., Portin, H., Wiedensohler, A., Weinhold, K., Merkel, M., Tuch, T., and Harrison, R. M.: The effect of meteorological conditions and atmospheric composition in the occurrence and development of new particle formation (NPF) events in Europe, *ACP*, 21, 3345–3370, 10.5194/acp-21-3345-2021, 2021.
- 720 Cai, M., Liang, B., Sun, Q., Liu, L., Yuan, B., Shao, M., Huang, S., Peng, Y., Wang, Z., Tan, H., Li, F., Xu, H., Chen, D., and Zhao, J.: The important roles of surface tension and growth rate in the contribution of new particle formation (NPF) to cloud condensation nuclei (CCN) number concentration: evidence from field measurements in southern China, *ACP*, 21, 8575–8592, 10.5194/acp-21-8575-2021, 2021a.
- Cai, R., Chen, D.-R., Hao, J., and Jiang, J.: A miniature cylindrical differential mobility analyzer for sub-3 nm particle sizing, *Journal of Aerosol Science*, 106, 111–119, 10.1016/j.jaerosci.2017.01.004, 2017a.
- 725 Cai, R., Häkkinen, E., Yan, C., Jiang, J., Kulmala, M., and Kangasluoma, J.: The effectiveness of the coagulation sink of 3–10 nm atmospheric particles, *ACP*, 22, 11529–11541, 10.5194/acp-22-11529-2022, 2022a.



- Cai, R., Yang, D., Fu, Y., Wang, X., Li, X., Ma, Y., Hao, J., Zheng, J., and Jiang, J.: Aerosol surface area concentration: a governing factor in new particle formation in Beijing, *ACP*, 17, 12327-12340, 10.5194/acp-17-12327-2017, 2017b.
- 730 Cai, R., Yan, C., Worsnop, D. R., Bianchi, F., Kerminen, V.-M., Liu, Y., Wang, L., Zheng, J., Kulmala, M., and Jiang, J.: An indicator for sulfuric acid–amine nucleation in atmospheric environments, *Aerosol Science and Technology*, 55, 1059-1069, 10.1080/02786826.2021.1922598, 2021b.
- Cai, R., Li, C., He, X.-C., Deng, C., Lu, Y., Yin, R., Yan, C., Wang, L., Jiang, J., Kulmala, M., and Kangasluoma, J.: Impacts of coagulation on the appearance time method for new particle growth rate evaluation and their corrections, *ACP*, 21, 2287-2304, 10.5194/acp-21-2287-2021, 2021c.
- 735 Cai, R., Yan, C., Yang, D., Yin, R., Lu, Y., Deng, C., Fu, Y., Ruan, J., Li, X., Kontkanen, J., Zhang, Q., Kangasluoma, J., Ma, Y., Hao, J., Worsnop, D. R., Bianchi, F., Paasonen, P., Kerminen, V.-M., Liu, Y., Wang, L., Zheng, J., Kulmala, M., and Jiang, J.: Sulfuric acid–amine nucleation in urban Beijing, *ACP*, 21, 2457-2468, 10.5194/acp-21-2457-2021, 2021d.
- Cai, R., Yin, R., Yan, C., Yang, D., Deng, C., Dada, L., Kangasluoma, J., Kontkanen, J., Halonen, R., Ma, Y., Zhang, X., Paasonen, P., Petäjä, T., Kerminen, V. M., Liu, Y., Bianchi, F., Zheng, J., Wang, L., Hao, J., Smith, J. N., Donahue, N. M., Kulmala, M., Worsnop, D. R., and Jiang, J.: The missing base molecules in atmospheric acid-base nucleation, *Natl Sci Rev*, 9, nwac137, 10.1093/nsr/nwac137, 2022b.
- 745 Carpenter, L. J., MacDonald, S. M., Shaw, M. D., Kumar, R., Saunders, R. W., Parthipan, R., Wilson, J., and Plane, J. M. C.: Atmospheric iodine levels influenced by sea surface emissions of inorganic iodine, *Nature Geoscience*, 6, 108-111, 10.1038/ngeo1687, 2013.
- Carpenter, L. J., Chance, R. J., Sherwen, T., Adams, T. J., Ball, S. M., Evans, M. J., Hepach, H., Hollis, L. D. J., Hughes, C., Jickells, T. D., Mahajan, A., Stevens, D. P., Tinel, L., and Wadley, M. R.: Marine iodine emissions in a changing world, *Proceedings of the Royal Society A: Mathematical, Physical and Engineering Sciences*, 477, 10.1098/rspa.2020.0824, 2021.
- 750 Chen, R., Hu, B., Liu, Y., Xu, J., Yang, G., Xu, D., and Chen, C.: Beyond PM_{2.5}: The role of ultrafine particles on adverse health effects of air pollution, *Biochimica et Biophysica Acta (BBA) - General Subjects*, 1860, 2844-2855, 10.1016/j.bbagen.2016.03.019, 2016.
- 755 Chen, Y., Liu, S., Yang, G., and He, Z.: Influence Factors on Photochemical Production of Methyl Iodide in Seawater, *Journal of Ocean University of China*, 19, 1353-1361, 10.1007/s11802-020-4463-8, 2020.
- Chu, B., Kerminen, V. M., Bianchi, F., Yan, C., Petäjä, T., and Kulmala, M.: Atmospheric new particle formation in China, *Atmos. Chem. Phys.*, 19, 115-138, 10.5194/acp-19-115-2019, 2019.
- Claudio Tomasi, S. F., and Alexander Kokhanovsky: *Atmospheric Aerosols: Life Cycles and Effects on Air Quality and Climate*, 1-86 pp.2017.
- 760 Dada, L., Lehtipalo, K., Kontkanen, J., Nieminen, T., Baalbaki, R., Ahonen, L., Duplissy, J., Yan, C., Chu, B., Petäjä, T., Lehtinen, K., Kerminen, V.-M., Kulmala, M., and Kangasluoma, J.: Formation and growth of sub-3-nm aerosol particles in experimental chambers, *Nature Protocols*, 15, 1013-1040, 10.1038/s41596-019-0274-z, 2020.
- 765 Deng, C., Cai, R., Yan, C., Zheng, J., and Jiang, J.: Formation and growth of sub-3 nm particles in megacities: impact of background aerosols, *Faraday Discuss*, 226, 348-363, 10.1039/d0fd00083c, 2020a.
- Deng, C., Fu, Y., Dada, L., Yan, C., Cai, R., Yang, D., Zhou, Y., Yin, R., Lu, Y., Li, X., Qiao, X., Fan, X., Nie, W., Kontkanen, J., Kangasluoma, J., Chu, B., Ding, A., Kerminen, V. M., Paasonen, P., Worsnop, D. R., Bianchi, F., Liu, Y., Zheng, J., Wang, L., Kulmala, M., and Jiang, J.: Seasonal Characteristics of New Particle Formation and Growth in Urban Beijing, *EST*, 54, 8547-8557, 10.1021/acs.est.0c00808, 2020b.
- 770



- Dimmer, C. H., Simmonds, P. G., Nickless, G., and Bassford, M. R. J. A. E.: Biogenic fluxes of halomethanes from Irish peatland ecosystems, *Atmospheric Environment*, 35, 321-330, Doi 10.1016/S1352-2310(00)00151-5, 2001.
- 775 Ding, A., Nie, W., Huang, X., Chi, X., Sun, J., Kerminen, V.-M., Xu, Z., Guo, W., Petäjä, T., Yang, X., Kulmala, M., and Fu, C.: Long-term observation of air pollution-weather/climate interactions at the SORPES station: a review and outlook, *Frontiers of Environmental Science & Engineering*, 10, 15, 10.1007/s11783-016-0877-3, 2016.
- Ding, A., Huang, X., Nie, W., Chi, X., Xu, Z., Zheng, L., Xu, Z., Xie, Y., Qi, X., Shen, Y., Sun, P., 780 Wang, J., Wang, L., Sun, J., Yang, X.-Q., Qin, W., Zhang, X., Cheng, W., Liu, W., Pan, L., and Fu, C.: Significant reduction of PM_{2.5} in eastern China due to regional-scale emission control: evidence from SORPES in 2011–2018, *ACP*, 19, 11791-11801, 10.5194/acp-19-11791-2019, 2019.
- Downward, G. S., van Nunen, E., Kerckhoffs, J., Vineis, P., Brunekreef, B., Boer, J. M. A., Messier, K. P., Roy, A., Verschuren, W. M. M., van der Schouw, Y. T., Sluijs, I., Gulliver, J., Hoek, G., and 785 Vermeulen, R.: Long-Term Exposure to Ultrafine Particles and Incidence of Cardiovascular and Cerebrovascular Disease in a Prospective Study of a Dutch Cohort, *Environmental Health Perspectives*, 126, 127007, 10.1289/EHP3047, 2018.
- Drougas, E. and Kosmas, A. M. J. T. J. o. P. C. A.: Computational studies of (HIO₃) isomers and the HO₂+ IO reaction pathways, 109, 3887-3892, 2005.
- 790 Ehn, M., Thornton, J. A., Kleist, E., Sipilä, M., Junninen, H., Pullinen, I., Springer, M., Rubach, F., Tillmann, R., Lee, B., Lopez-Hilfiker, F., Andres, S., Acir, I.-H., Rissanen, M., Jokinen, T., Schobesberger, S., Kangasluoma, J., Kontkanen, J., Nieminen, T., Kurtén, T., Nielsen, L. B., Jørgensen, S., Kjaergaard, H. G., Canagaratna, M., Maso, M. D., Berndt, T., Petäjä, T., Wahner, A., Kerminen, V.-M., Kulmala, M., Worsnop, D. R., Wildt, J., and Mentel, T. F.: A large source of low-volatility secondary 795 organic aerosol, *Nature*, 506, 476-479, 10.1038/nature13032, 2014.
- Finkenzeller, H., Iyer, S., He, X.-C., Simon, M., Koenig, T. K., Lee, C. F., Valiev, R., Hofbauer, V., Amorim, A., Baalbaki, R., Baccarini, A., Beck, L., Bell, D. M., Caudillo, L., Chen, D., Chiu, R., Chu, B., Dada, L., Duplissy, J., Heinritzi, M., Kempainen, D., Kim, C., Krechmer, J., Kürten, A., Kvashnin, A., Lamkaddam, H., Lee, C. P., Lehtipalo, K., Li, Z., Makhmutov, V., Manninen, H. E., Marie, G., 800 Marten, R., Mauldin, R. L., Mentler, B., Müller, T., Petäjä, T., Philippov, M., Ranjithkumar, A., Rörup, B., Shen, J., Stolzenburg, D., Tauber, C., Tham, Y. J., Tomé, A., Vazquez-Pufleau, M., Wagner, A. C., Wang, D. S., Wang, M., Wang, Y., Weber, S. K., Nie, W., Wu, Y., Xiao, M., Ye, Q., Zauner-Wieczorek, M., Hansel, A., Baltensperger, U., Brioude, J., Curtius, J., Donahue, N. M., Haddad, I. E., Flagan, R. C., Kulmala, M., Kirkby, J., Sipilä, M., Worsnop, D. R., Kurten, T., Rissanen, M., and Volkamer, R.: The 805 gas-phase formation mechanism of iodic acid as an atmospheric aerosol source, *Nature Chemistry*, 15, 129-135, 10.1038/s41557-022-01067-z, 2023.
- Gomez Martin, J. C., Lewis, T. R., Blitz, M. A., Plane, J. M. C., Kumar, M., Francisco, J. S., and Saiz-Lopez, A.: A gas-to-particle conversion mechanism helps to explain atmospheric particle formation through clustering of iodine oxides, *Nature Communications*, 11, 4521, 10.1038/s41467-020-18252-8, 810 2020.
- Guo, Y., Yan, C., Li, C., Ma, W., Feng, Z., Zhou, Y., Lin, Z., Dada, L., Stolzenburg, D., Yin, R., Kontkanen, J., Daellenbach, K. R., Kangasluoma, J., Yao, L., Chu, B., Wang, Y., Cai, R., Bianchi, F., Liu, Y., and Kulmala, M.: Formation of nighttime sulfuric acid from the ozonolysis of alkenes in Beijing, *ACP*, 21, 5499-5511, 10.5194/acp-21-5499-2021, 2021.



- 815 He, X.-C., Iyer, S., Sipilä, M., Ylisirniö, A., Peltola, M., Kontkanen, J., Baalbaki, R., Simon, M., Kürten, A., Tham, Y. J., Pesonen, J., Ahonen, L. R., Amanatidis, S., Amorim, A., Baccarini, A., Beck, L., Bianchi, F., Brilke, S., Chen, D., Chiu, R., Curtius, J., Dada, L., Dias, A., Dommen, J., Donahue, N. M., Duplissy, J., El Haddad, I., Finkenzeller, H., Fischer, L., Heinritzi, M., Hofbauer, V., Kangasluoma, J., Kim, C., Koenig, T. K., Kubečka, J., Kvashnin, A., Lamkaddam, H., Lee, C. P., Leiminger, M., Li, Z.,
- 820 Makhmutov, V., Xiao, M., Marten, R., Nie, W., Onnela, A., Partoll, E., Petäjä, T., Salo, V.-T., Schuchmann, S., Steiner, G., Stolzenburg, D., Stozhkov, Y., Tauber, C., Tomé, A., Väisänen, O., Vazquez-Pufleau, M., Volkamer, R., Wagner, A. C., Wang, M., Wang, Y., Wimmer, D., Winkler, P. M., Worsnop, D. R., Wu, Y., Yan, C., Ye, Q., Lehtinen, K., Nieminen, T., Manninen, H. E., Rissanen, M., Schobesberger, S., Lehtipalo, K., Baltensperger, U., Hansel, A., Kerminen, V.-M., Flagan, R. C., Kirkby, J., Kurtén, T., and Kulmala, M.: Determination of the collision rate coefficient between charged iodine acid clusters and iodine acid using the appearance time method, *Aerosol Science and Technology*, 55, 231-242, 10.1080/02786826.2020.1839013, 2021a.
- He, X.: From the measurement of halogenated species to iodine particle formation, 2017.
- He, X. C., Tham, Y. J., Dada, L., Wang, M., Finkenzeller, H., Stolzenburg, D., Iyer, S., Simon, M.,
- 830 Kürten, A., Shen, J., Rörup, B., Rissanen, M., Schobesberger, S., Baalbaki, R., Wang, D. S., Koenig, T. K., Jokinen, T., Sarnela, N., Beck, L. J., Almeida, J., Amanatidis, S., Amorim, A., Ataei, F., Baccarini, A., Bertozzi, B., Bianchi, F., Brilke, S., Caudillo, L., Chen, D., Chiu, R., Chu, B., Dias, A., Ding, A., Dommen, J., Duplissy, J., El Haddad, I., Gonzalez Carracedo, L., Granzin, M., Hansel, A., Heinritzi, M., Hofbauer, V., Junninen, H., Kangasluoma, J., Kempainen, D., Kim, C., Kong, W., Krechmer, J. E.,
- 835 Kvashin, A., Laitinen, T., Lamkaddam, H., Lee, C. P., Lehtipalo, K., Leiminger, M., Li, Z., Makhmutov, V., Manninen, H. E., Marie, G., Marten, R., Mathot, S., Mauldin, R. L., Mentler, B., Möhler, O., Müller, T., Nie, W., Onnela, A., Petäjä, T., Pfeifer, J., Philippov, M., Ranjithkumar, A., Saiz-Lopez, A., Salma, I., Scholz, W., Schuchmann, S., Schulze, B., Steiner, G., Stozhkov, Y., Tauber, C., Tomé, A., Thakur, R. C., Väisänen, O., Vazquez-Pufleau, M., Wagner, A. C., Wang, Y., Weber, S. K., Winkler, P. M., Wu,
- 840 Y., Xiao, M., Yan, C., Ye, Q., Ylisirniö, A., Zauner-Wieczorek, M., Zha, Q., Zhou, P., Flagan, R. C., Curtius, J., Baltensperger, U., Kulmala, M., Kerminen, V. M., Kurtén, T., Donahue, N. M., Volkamer, R., Kirkby, J., Worsnop, D. R., and Sipilä, M.: Role of iodine oxoacids in atmospheric aerosol nucleation, *Science*, 371, 589-595, 10.1126/science.abe0298, 2021b.
- Hoffmann, T., O'Dowd, C. D., and Seinfeld, J. H.: Iodine oxide homogeneous nucleation: An explanation
- 845 for coastal new particle production, *GRL*, 28, 1949-1952, 10.1029/2000gl012399, 2001.
- Jiang, J., Chen, M., Kuang, C., Attoui, M., and McMurry, P. H.: Electrical Mobility Spectrometer Using a Diethylene Glycol Condensation Particle Counter for Measurement of Aerosol Size Distributions Down to 1 nm, *Aerosol Science and Technology*, 45, 510-521, 10.1080/02786826.2010.547538, 2011.
- Jimenez, J. L.: New particle formation from photooxidation of diiodomethane (CH₂I₂), *Journal of Geophysical Research*, 108, 10.1029/2002jd002452, 2003.
- Jokinen, T., Lehtipalo, K., Thakur, R. C., Ylivinkka, I., Neitola, K., Sarnela, N., Laitinen, T., Kulmala, M., Petäjä, T., and Sipilä, M.: Measurement report: Long-term measurements of aerosol precursor concentrations in the Finnish subarctic boreal forest, *ACP*, 22, 2237-2254, 10.5194/acp-22-2237-2022, 2022.
- 855 Jokinen, T., Sipilä, M., Junninen, H., Ehn, M., Lönn, G., Hakala, J., Petäjä, T., Mauldin, R. L., Kulmala, M., and Worsnop, D. R.: Atmospheric sulphuric acid and neutral cluster measurements using CI-API-TOF, *ACP*, 12, 4117-4125, 10.5194/acp-12-4117-2012, 2012.



- Jokinen, T., Sipilä, M., Kontkanen, J., Vakkari, V., Tisler, P., Duplissy, E.-M., Junninen, H., Kangasluoma, J., Manninen, H., and Petäjä, T. J. S. A.: Ion-induced sulfuric acid–ammonia nucleation drives particle formation in coastal Antarctica, *Science Advances*, 4, eaat9744, 2018.
- 860 Junninen, H., Ehn, M., Petäjä, T., Luosujärvi, L., Kotiaho, T., Kostianinen, R., Rohner, U., Gonin, M., Fuhrer, K., Kulmala, M., and Worsnop, D. R.: A high-resolution mass spectrometer to measure atmospheric ion composition, *Atmospheric Measurement Techniques*, 3, 1039-1053, 10.5194/amt-3-1039-2010, 2010.
- 865 Kalkavouras, P., Bossioli, E., Bezantakos, S., Bougiatioti, A., Kalivitis, N., Stavroulas, I., Kouvarakis, G., Protonotariou, A. P., Dandou, A., Biskos, G., Mihalopoulos, N., Nenes, A., and Tombrou, M.: New particle formation in the southern Aegean Sea during the Etesians: importance for CCN production and cloud droplet number, *ACP*, 17, 175-192, 10.5194/acp-17-175-2017, 2017.
- Kerminen, V.-M., Lihavainen, H., Komppula, M., Viisanen, Y., and Kulmala, M.: Direct observational evidence linking atmospheric aerosol formation and cloud droplet activation, *GRL*, 32, 10.1029/2005gl023130, 2005.
- 870 Kerminen, V.-M., Chen, X., Vakkari, V., Petäjä, T., Kulmala, M., and Bianchi, F.: Atmospheric new particle formation and growth: review of field observations, *ERL*, 13, 10.1088/1748-9326/aadf3c, 2018.
- Kirkby, J., Curtius, J., Almeida, J., Dunne, E., Duplissy, J., Ehrhart, S., Franchin, A., Gagné, S., Ickes, L., Kürten, A., Kupc, A., Metzger, A., Riccobono, F., Rondo, L., Schobesberger, S., Tsagkogeorgas, G., Wimmer, D., Amorim, A., Bianchi, F., Breitenlechner, M., David, A., Dommen, J., Downard, A., Ehn, M., Flagan, R. C., Haider, S., Hansel, A., Hauser, D., Jud, W., Junninen, H., Kreissl, F., Kvashin, A., Laaksonen, A., Lehtipalo, K., Lima, J., Lovejoy, E. R., Makhmutov, V., Mathot, S., Mikkilä, J., Minginette, P., Mogo, S., Nieminen, T., Onnela, A., Pereira, P., Petäjä, T., Schnitzhofer, R., Seinfeld, J.
- 880 H., Sipilä, M., Stozhkov, Y., Stratmann, F., Tomé, A., Vanhanen, J., Viisanen, Y., Vrtala, A., Wagner, P. E., Walther, H., Weingartner, E., Wex, H., Winkler, P. M., Carslaw, K. S., Worsnop, D. R., Baltensperger, U., and Kulmala, M.: Role of sulphuric acid, ammonia and galactic cosmic rays in atmospheric aerosol nucleation, *Nature*, 476, 429-433, 10.1038/nature10343, 2011.
- Kirkby, J., Duplissy, J., Sengupta, K., Frege, C., Gordon, H., Williamson, C., Heinritzi, M., Simon, M., Yan, C., Almeida, J., Tröstl, J., Nieminen, T., Ortega, I. K., Wagner, R., Adamov, A., Amorim, A., Bernhammer, A.-K., Bianchi, F., Breitenlechner, M., Brilke, S., Chen, X., Craven, J., Dias, A., Ehrhart, S., Flagan, R. C., Franchin, A., Fuchs, C., Guida, R., Hakala, J., Hoyle, C. R., Jokinen, T., Junninen, H., Kangasluoma, J., Kim, J., Krapf, M., Kürten, A., Laaksonen, A., Lehtipalo, K., Makhmutov, V., Mathot, S., Molteni, U., Onnela, A., Peräkylä, O., Piel, F., Petäjä, T., Praplan, A. P., Pringle, K., Rap, A.,
- 890 Richards, N. A. D., Riipinen, I., Rissanen, M. P., Rondo, L., Sarnela, N., Schobesberger, S., Scott, C. E., Seinfeld, J. H., Sipilä, M., Steiner, G., Stozhkov, Y., Stratmann, F., Tomé, A., Virtanen, A., Vogel, A. L., Wagner, A. C., Wagner, P. E., Weingartner, E., Wimmer, D., Winkler, P. M., Ye, P., Zhang, X., Hansel, A., Dommen, J., Donahue, N. M., Worsnop, D. R., Baltensperger, U., Kulmala, M., Carslaw, K. S., and Curtius, J.: Ion-induced nucleation of pure biogenic particles, *Nature*, 533, 521-526, 10.1038/nature17953, 2016.
- 895 Kuang, C., Riipinen, I., Sihto, S. L., Kulmala, M., McCormick, A. V., and McMurry, P. H.: An improved criterion for new particle formation in diverse atmospheric environments, *ACP*, 10, 8469-8480, 10.5194/acp-10-8469-2010, 2010.
- Kulmala, M., Kerminen, V. M., Anttila, T., Laaksonen, A., and O'Dowd, C. D.: Organic aerosol formation via sulphate cluster activation, *Journal of Geophysical Research: Atmospheres*, 109, Artn D0420510.1029/2003jd003961, 2004a.
- 900



- Kulmala, M., Kerminen, V. M., Petäjä, T., Ding, A. J., and Wang, L.: Atmospheric gas-to-particle conversion: why NPF events are observed in megacities?, *Faraday Discuss*, 200, 271-288, 10.1039/c6fd00257a, 2017.
- 905 Kulmala, M., Vehkamäki, H., Petäjä, T., Dal Maso, M., Lauri, A., Kerminen, V. M., Birmili, W., and McMurry, P. H.: Formation and growth rates of ultrafine atmospheric particles: a review of observations, *Journal of Aerosol Science*, 35, 143-176, 10.1016/j.jaerosci.2003.10.003, 2004b.
- Kulmala, M., Maso, M. D., Mäkelä, J., Pirjola, L., Väkevä, M., Aalto, P., Miiikkulainen, P., Hämeri, K., and O'dowd, C. J. T. B.: On the formation, growth and composition of nucleation mode particles, 53, 479-490, 2001.
- 910 Kulmala, M., Cai, R., Stolzenburg, D., Zhou, Y., Dada, L., Guo, Y., Yan, C., Petäjä, T., Jiang, J., and Kerminen, V. M.: The contribution of new particle formation and subsequent growth to haze formation, *Environ Sci Atmos*, 2, 352-361, 10.1039/d1ea00096a, 2022.
- Kulmala, M., Petäjä, T., Nieminen, T., Sipilä, M., Manninen, H. E., Lehtipalo, K., Dal Maso, M., Aalto, P. P., Junninen, H., Paasonen, P., Riipinen, I., Lehtinen, K. E., Laaksonen, A., and Kerminen, V. M.: Measurement of the nucleation of atmospheric aerosol particles, *Nature Protocols*, 7, 1651-1667, 10.1038/nprot.2012.091, 2012.
- 915 Kulmala, M., Dada, L., Däellenbach, K. R., Yan, C., Stolzenburg, D., Kontkanen, J., Ezhova, E., Hakala, S., Tuovinen, S., Kokkonen, T. V., Kurppa, M., Cai, R., Zhou, Y., Yin, R., Baalbaki, R., Chan, T., Chu, B., Deng, C., Fu, Y., Ge, M., He, H., Heikkinen, L., Junninen, H., Liu, Y., Lu, Y., Nie, W., Rusanen, A., Vakkari, V., Wang, Y., Yang, G., Yao, L., Zheng, J., Kujansuu, J., Kangasluoma, J., Petäjä, T., Paasonen, P., Jarvi, L., Worsnop, D., Ding, A., Liu, Y., Wang, L., Jiang, J., Bianchi, F., and Kerminen, V. M.: Is reducing new particle formation a plausible solution to mitigate particulate air pollution in Beijing and other Chinese megacities?, *Faraday Discuss*, 226, 334-347, 10.1039/d0fd00078g, 2021.
- 925 Kürten, A., Bergen, A., Heinritzi, M., Leiminger, M., Lorenz, V., Piel, F., Simon, M., Sitals, R., Wagner, A. C., and Curtius, J.: Observation of new particle formation and measurement of sulfuric acid, ammonia, amines and highly oxidized organic molecules at a rural site in central Germany, *ACP*, 16, 12793-12813, 10.5194/acp-16-12793-2016, 2016.
- Laakso, L., Petäjä, T., Lehtinen, K. E. J., Kulmala, M., Paatero, J., Hörrak, U., Tammets, H., and Joutsensaari, J.: Ion production rate in a boreal forest based on ion, particle and radiation measurements, *ACP*, 4, 1933-1943, DOI 10.5194/acp-4-1933-2004, 2004.
- 930 Lehtinen, K., Korhonen, H., Maso, M. D., and Kulmala, M. J. B. E. R.: On the concept of condensation sink diameter, 8, 405-411, 2003.
- Lehtinen, K. E. J., Dal Maso, M., Kulmala, M., and Kerminen, V.-M.: Estimating nucleation rates from apparent particle formation rates and vice versa: Revised formulation of the Kerminen–Kulmala equation, *Journal of Aerosol Science*, 38, 988-994, 10.1016/j.jaerosci.2007.06.009, 2007.
- 935 Lehtipalo, K., Kontkanen, J., Kangasluoma, J., Franchin, A., and Research, J. L. J. B. E.: Methods for determining particle size distribution and growth rates between 1 and 3 nm using the Particle Size Magnifier, 19, 215-236, 2014.
- 940 Lehtipalo, K., Yan, C., Dada, L., Bianchi, F., Xiao, M., Wagner, R., Stolzenburg, D., Ahonen, L. R., Amorim, A., Baccarini, A., Bauer, P. S., Baumgartner, B., Bergen, A., Bernhammer, A. K., Breitenlechner, M., Brilke, S., Buchholz, A., Mazon, S. B., Chen, D., Chen, X., Dias, A., Dommen, J., Draper, D. C., Duplissy, J., Ehn, M., Finkenzeller, H., Fischer, L., Frege, C., Fuchs, C., Garmash, O., Gordon, H., Hakala, J., He, X., Heikkinen, L., Heinritzi, M., Helm, J. C., Hofbauer, V., Hoyle, C. R., Jokinen, T., Kangasluoma, J., Kerminen, V. M., Kim, C., Kirkby, J., Kontkanen, J., Kürten, A., Lawler,
- 945



- M. J., Mai, H., Mathot, S., Mauldin, R. L., 3rd, Molteni, U., Nichman, L., Nie, W., Nieminen, T., Ojdic, A., Onnela, A., Passananti, M., Petäjä, T., Piel, F., Pospisilova, V., Quéléver, L. L. J., Rissanen, M. P., Rose, C., Sarnela, N., Schallhart, S., Schuchmann, S., Sengupta, K., Simon, M., Sipilä, M., Tauber, C., Tomé, A., Tröstl, J., Väisänen, O., Vogel, A. L., Volkamer, R., Wagner, A. C., Wang, M., Weitz, L.,
950 Wimmer, D., Ye, P., Ylisirniö, A., Zha, Q., Carslaw, K. S., Curtius, J., Donahue, N. M., Flagan, R. C., Hansel, A., Riipinen, I., Virtanen, A., Winkler, P. M., Baltensperger, U., Kulmala, M., and Worsnop, D. R.: Multicomponent new particle formation from sulfuric acid, ammonia, and biogenic vapors, *Sci Adv*, 4, eaau5363, 10.1126/sciadv.aau5363, 2018.
- Li, H., Ning, A., Zhong, J., Zhang, H., Liu, L., Zhang, Y., Zhang, X., Zeng, X. C., and He, H.: Influence
955 of atmospheric conditions on sulfuric acid-dimethylamine-ammonia-based new particle formation, *Chemosphere*, 245, 125554, 10.1016/j.chemosphere.2019.125554, 2020.
- Li, Y., He, Z., Yang, G. P., and Zou, Y.: Spatial distribution and biogeochemical cycling of methyl iodide in the Yellow Sea and the East China Sea during summer, *Environmental Pollution*, 276, 116749, 10.1016/j.envpol.2021.116749, 2021.
- 960 Li, Y., Chi, L., Mao, L., Yan, D., Wu, Z., Ma, T., Guo, M., Wang, Q., Ouyang, C., and Cao, A.: Control of Soilborne Pathogens of *Zingiber officinale* by Methyl Iodide and Chloropicrin in China, *Plant Dis*, 98, 384-388, 10.1094/PDIS-06-13-0623-RE, 2014.
- Liu, J., Jiang, J., Zhang, Q., Deng, J., and Hao, J.: A spectrometer for measuring particle size distributions in the range of 3 nm to 10 μ m, *Frontiers of Environmental Science & Engineering*, 10, 63-72,
965 10.1007/s11783-014-0754-x, 2016.
- Liu, Y., Yan, C., Feng, Z., Zheng, F., Fan, X., Zhang, Y., Li, C., Zhou, Y., Lin, Z., Guo, Y., Zhang, Y., Ma, L., Zhou, W., Liu, Z., Dada, L., Dällenbach, K., Kontkanen, J., Cai, R., Chan, T., Chu, B., Du, W., Yao, L., Wang, Y., Cai, J., Kangasluoma, J., Kokkonen, T., Kujansuu, J., Rusanen, A., Deng, C., Fu, Y., Yin, R., Li, X., Lu, Y., Liu, Y., Lian, C., Yang, D., Wang, W., Ge, M., Wang, Y., Worsnop, D. R.,
970 Junninen, H., He, H., Kerminen, V.-M., Zheng, J., Wang, L., Jiang, J., Petäjä, T., Bianchi, F., and Kulmala, M.: Continuous and comprehensive atmospheric observations in Beijing: a station to understand the complex urban atmospheric environment, *Big Earth Data*, 4, 295-321, 10.1080/20964471.2020.1798707, 2020.
- Lu, Y., Yan, C., Fu, Y., Chen, Y., Liu, Y., Yang, G., Wang, Y., Bianchi, F., Chu, B., Zhou, Y., Yin, R.,
975 Baalbaki, R., Garmash, O., Deng, C., Wang, W., Liu, Y., Petäjä, T., Kerminen, V.-M., Jiang, J., Kulmala, M., and Wang, L.: A proxy for atmospheric daytime gaseous sulfuric acid concentration in urban Beijing, *ACP*, 19, 1971-1983, 10.5194/acp-19-1971-2019, 2019.
- Mäkelä, J. M.: Biogenic iodine emissions and identification of end-products in coastal ultrafine particles during nucleation bursts, *Journal of Geophysical Research*, 107, 10.1029/2001jd000580, 2002.
- 980 Manninen, H. E., Mirme, S., Mirme, A., Petäjä, T., and Kulmala, M.: How to reliably detect molecular clusters and nucleation mode particles with Neutral cluster and Air Ion Spectrometer (NAIS), *Atmospheric Measurement Techniques*, 9, 3577-3605, 10.5194/amt-9-3577-2016, 2016.
- McMurry, P. H., Fink, M., Sakurai, H., Stolzenburg, M. R., Mauldin, R. L., Smith, J., Eisele, F., Moore, K., Sjostedt, S., Tanner, D., Huey, L. G., Nowak, J. B., Edgerton, E., and Voisin, D.: A criterion for new
985 particle formation in the sulfur-rich Atlanta atmosphere, *Journal of Geophysical Research*, 110, 10.1029/2005jd005901, 2005.
- Moore, R. M. and Zafiriou, O. C.: Photochemical Production of Methyl-Iodide in Seawater, *J Geophys Res-Atmos*, 99, 16415-16420, Doi 10.1029/94jd00786, 1994.



- Nie, W., Yan, C., Huang, D. D., Wang, Z., Liu, Y., Qiao, X., Guo, Y., Tian, L., Zheng, P., Xu, Z., Li, Y.,
990 Xu, Z., Qi, X., Sun, P., Wang, J., Zheng, F., Li, X., Yin, R., Dallenbach, K. R., Bianchi, F., Petäjä, T.,
Zhang, Y., Wang, M., Schervish, M., Wang, S., Qiao, L., Wang, Q., Zhou, M., Wang, H., Yu, C., Yao,
D., Guo, H., Ye, P., Lee, S., Li, Y. J., Liu, Y., Chi, X., Kerminen, V.-M., Ehn, M., Donahue, N. M.,
Wang, T., Huang, C., Kulmala, M., Worsnop, D., Jiang, J., and Ding, A.: Secondary organic aerosol
995 10.1038/s41561-022-00922-5, 2022.
- Nieminen, T., Lehtinen, K. E. J., and Kulmala, M.: Sub-10 nm particle growth by vapor condensation –
effects of vapor molecule size and particle thermal speed, *ACP*, 10, 9773-9779, 10.5194/acp-10-9773-
2010, 2010.
- Ning, A., Liu, L., Zhang, S., Yu, F., Du, L., Ge, M., and Zhang, X.: The critical role of dimethylamine
1000 in the rapid formation of iodic acid particles in marine areas, *npj Climate and Atmospheric Science*, 5,
92, 10.1038/s41612-022-00316-9, 2022.
- O'Dowd, C. D. and Hoffmann, T.: Coastal New Particle Formation: A Review of the Current State-Of-
The-Art, *Environmental Chemistry*, 2, 10.1071/en05077, 2005.
- O'Dowd, C. D., Jimenez, J. L., Bahreini, R., Flagan, R. C., Seinfeld, J. H., Hämeri, K., Pirjola, L.,
1005 Kulmala, M., Jennings, S. G., and Hoffmann, T.: Marine aerosol formation from biogenic iodine
emissions, *Nature*, 417, 632-636, 10.1038/nature00775, 2002.
- Paasonen, P., Peltola, M., Kontkanen, J., Junninen, H., Kerminen, V.-M., and Kulmala, M.:
Comprehensive analysis of particle growth rates from nucleation mode to cloud condensation nuclei in
boreal forest, *ACP*, 18, 12085-12103, 10.5194/acp-18-12085-2018, 2018.
- 1010 Paasonen, P., Asmi, A., Petäjä, T., Kajos, M. K., Äijälä, M., Junninen, H., Holst, T., Abbatt, J. P. D.,
Arneth, A., Birmili, W., van der Gon, H. D., Hamed, A., Hoffer, A., Laakso, L., Laaksonen, A., Richard
Leitch, W., Plass-Dülmer, C., Pryor, S. C., Räisänen, P., Swietlicki, E., Wiedensohler, A., Worsnop, D.
R., Kerminen, V.-M., and Kulmala, M.: Warming-induced increase in aerosol number concentration
likely to moderate climate change, *Nature Geoscience*, 6, 438-442, 10.1038/ngeo1800, 2013.
- 1015 Petäjä, T., Mauldin, I. R. L., Kosciuch, E., McGrath, J., Nieminen, T., Paasonen, P., Boy, M., Adamov,
A., Kotiaho, T., and Kulmala, M.: Sulfuric acid and OH concentrations in a boreal forest site, *Atmos.
Chem. Phys.*, 9, 7435-7448, 10.5194/acp-9-7435-2009, 2009.
- Plane, J., Joseph, D., Allan, B., Ashworth, S., and Francisco, J. J. T. J. o. P. C. A.: An experimental and
theoretical study of the reactions $\text{OIO} + \text{NO}$ and $\text{OIO} + \text{OH}$, 110, 93-100, 2006.
- 1020 Qi, X. M., Ding, A. J., Nie, W., Petäjä, T., Kerminen, V. M., Herrmann, E., Xie, Y. N., Zheng, L. F.,
Manninen, H., Aalto, P., Sun, J. N., Xu, Z. N., Chi, X. G., Huang, X., Boy, M., Virkkula, A., Yang, X.
Q., Fu, C. B., and Kulmala, M.: Aerosol size distribution and new particle formation in the western
Yangtze River Delta of China: 2 years of measurements at the SORPES station, *ACP*, 15, 12445-12464,
10.5194/acp-15-12445-2015, 2015.
- 1025 Qiao, X., Yan, C., Li, X., Guo, Y., Yin, R., Deng, C., Li, C., Nie, W., Wang, M., Cai, R., Huang, D.,
Wang, Z., Yao, L., Worsnop, D. R., Bianchi, F., Liu, Y., Donahue, N. M., Kulmala, M., and Jiang, J.:
Contribution of Atmospheric Oxygenated Organic Compounds to Particle Growth in an Urban
Environment, *EST*, 55, 13646-13656, 10.1021/acs.est.1c02095, 2021.
- Redeker, K. R. and Cicerone, R. J.: Environmental controls over methyl halide emissions from rice
1030 paddies, *Global Biogeochemical Cycles*, 18, 10.1029/2003gb002092, 2004.



- Redeker, K. R., Wang, N., Low, J. C., McMillan, A., Tyler, S. C., and Cicerone, R. J.: Emissions of methyl halides and methane from rice paddies, *Science*, 290, 966-969, 10.1126/science.290.5493.966, 2000.
- 1035 Saiz-Lopez, A., Plane, J. M., Baker, A. R., Carpenter, L. J., von Glasow, R., Martin, J. C., McFiggans, G., and Saunders, R. W.: Atmospheric chemistry of iodine, *Chemical Reviews*, 112, 1773-1804, 10.1021/cr200029u, 2012.
- Shi, X., Qiu, X., Chen, Q., Chen, S., Hu, M., Rudich, Y., and Zhu, T.: Organic Iodine Compounds in Fine Particulate Matter from a Continental Urban Region: Insights into Secondary Formation in the Atmosphere, *EST*, 55, 1508-1514, 10.1021/acs.est.0c06703, 2021.
- 1040 Sipilä, M., Sarnela, N., Jokinen, T., Henschel, H., Junninen, H., Kontkanen, J., Richters, S., Kangasluoma, J., Franchin, A., Peräkylä, O., Rissanen, M. P., Ehn, M., Vehkamäki, H., Kurten, T., Berndt, T., Petäjä, T., Worsnop, D., Ceburnis, D., Kerminen, V. M., Kulmala, M., and O'Dowd, C.: Molecular-scale evidence of aerosol particle formation via sequential addition of HIO₃, *Nature*, 537, 532-534, 10.1038/nature19314, 2016.
- 1045 Sive, B. C., Varner, R. K., Mao, H., Blake, D. R., Wingenter, O. W., and Talbot, R.: A large terrestrial source of methyl iodide, *GRL*, 34, 10.1029/2007gl030528, 2007.
- Stolzenburg, D., Simon, M., Ranjithkumar, A., Kürten, A., Lehtipalo, K., Gordon, H., Ehrhart, S., Finkenzeller, H., Pichelstorfer, L., Nieminen, T., He, X.-C., Brilke, S., Xiao, M., Amorim, A., Baalbaki, R., Baccarini, A., Beck, L., Bräkling, S., Caudillo Murillo, L., Chen, D., Chu, B., Dada, L., Dias, A., 1050 Dommen, J., Duplissy, J., El Haddad, I., Fischer, L., Gonzalez Carracedo, L., Heinritzi, M., Kim, C., Koenig, T. K., Kong, W., Lamkaddam, H., Lee, C. P., Leiminger, M., Li, Z., Makhmutov, V., Manninen, H. E., Marie, G., Marten, R., Müller, T., Nie, W., Partoll, E., Petäjä, T., Pfeifer, J., Philippov, M., Rissanen, M. P., Rörup, B., Schobesberger, S., Schuchmann, S., Shen, J., Sipilä, M., Steiner, G., Stozhkov, Y., Tauber, C., Tham, Y. J., Tomé, A., Vazquez-Pufleau, M., Wagner, A. C., Wang, M., Wang, 1055 Y., Weber, S. K., Wimmer, D., Wlasits, P. J., Wu, Y., Ye, Q., Zauner-Wieczorek, M., Baltensperger, U., Carslaw, K. S., Curtius, J., Donahue, N. M., Flagan, R. C., Hansel, A., Kulmala, M., Lelieveld, J., Volkamer, R., Kirkby, J., and Winkler, P. M.: Enhanced growth rate of atmospheric particles from sulfuric acid, *ACP*, 20, 7359-7372, 10.5194/acp-20-7359-2020, 2020.
- Thakur, R. C., Dada, L., Beck, L. J., Quéléver, L. L. J., Chan, T., Marbouti, M., He, X.-C., Xavier, C., 1060 Sulo, J., Lampilahti, J., Lampimäki, M., Tham, Y. J., Sarnela, N., Lehtipalo, K., Norkko, A., Kulmala, M., Sipilä, M., and Jokinen, T.: An evaluation of new particle formation events in Helsinki during a Baltic Sea cyanobacterial summer bloom, *ACP*, 22, 6365-6391, 10.5194/acp-22-6365-2022, 2022.
- Tröstl, J., Chuang, W. K., Gordon, H., Heinritzi, M., Yan, C., Molteni, U., Ahlm, L., Frege, C., Bianchi, F., Wagner, R., Simon, M., Lehtipalo, K., Williamson, C., Craven, J. S., Duplissy, J., Adamov, A., 1065 Almeida, J., Bernhammer, A.-K., Breitenlechner, M., Brilke, S., Dias, A., Ehrhart, S., Flagan, R. C., Franchin, A., Fuchs, C., Guida, R., Gysel, M., Hansel, A., Hoyle, C. R., Jokinen, T., Junninen, H., Kangasluoma, J., Keskinen, H., Kim, J., Krapf, M., Kürten, A., Laaksonen, A., Lawler, M., Leiminger, M., Mathot, S., Möhler, O., Nieminen, T., Onnela, A., Petäjä, T., Piel, F. M., Miettinen, P., Rissanen, M. P., Rondo, L., Sarnela, N., Schobesberger, S., Sengupta, K., Sipilä, M., Smith, J. N., Steiner, G., Tomé, 1070 A., Virtanen, A., Wagner, A. C., Weingartner, E., Wimmer, D., Winkler, P. M., Ye, P., Carslaw, K. S., Curtius, J., Dommen, J., Kirkby, J., Kulmala, M., Riipinen, I., Worsnop, D. R., Donahue, N. M., and Baltensperger, U.: The role of low-volatility organic compounds in initial particle growth in the atmosphere, *Nature*, 533, 527-531, 10.1038/nature18271, 2016.



- Veli-Matti Kerminen, M. K.: Analytical formulae connecting the “real” and the “apparent” nucleation rate and the nuclei number concentration for atmospheric nucleation events, *Journal of Aerosol Science*, 33, 609–622, 2002.
- 1075 Wang, Q., Yan, D., Wang, X., Lu, P., Li, X., and Cao, A.: Research advances in soil fumigants, *Acta Phytophylacica Sinica*, 44, 529-543, 2017.
- Wang, Z., Zheng, F., Zhang, W., and Wang, S.: Analysis of SO₂ Pollution Changes of Beijing-Tianjin-Hebei Region over China Based on OMI Observations from 2006 to 2017, *Advances in Meteorology*, 2018, 1-15, 10.1155/2018/8746068, 2018.
- 1080 Wehner, B., Siebert, H., Stratmann, F., Tuch, T., Wiedensohler, A., Petäjä, T., Dal Maso, M., and Kulmala, M.: Horizontal homogeneity and vertical extent of new particle formation events, *Tellus B: Chemical and Physical Meteorology*, 59, 362-371, 10.1111/j.1600-0889.2007.00260.x, 2007.
- 1085 Williams, J., Gros, V., Atlas, E., Maciejczyk, K., Batsaikhan, A., Schöler, H. F., Forster, C., Quack, B., Yassaa, N., Sander, R., and Van Dingenen, R.: Possible evidence for a connection between methyl iodide emissions and Saharan dust, *Journal of Geophysical Research*, 112, 10.1029/2005jd006702, 2007.
- Wu, Z., Hu, M., Liu, S., Wehner, B., Bauer, S., Maßling, A., Wiedensohler, A., Petäjä, T., Dal Maso, M., and Kulmala, M.: New particle formation in Beijing, China: Statistical analysis of a 1-year data set, *Journal of Geophysical Research*, 112, 10.1029/2006jd007406, 2007.
- 1090 Xiao, M., Hoyle, C. R., Dada, L., Stolzenburg, D., Kürten, A., Wang, M., Lamkaddam, H., Garmash, O., Mentler, B., Molteni, U., Baccarini, A., Simon, M., He, X.-C., Lehtipalo, K., Ahonen, L. R., Baalbaki, R., Bauer, P. S., Beck, L., Bell, D., Bianchi, F., Brilke, S., Chen, D., Chiu, R., Dias, A., Duplissy, J., Finkenzeller, H., Gordon, H., Hofbauer, V., Kim, C., Koenig, T. K., Lampilahti, J., Lee, C. P., Li, Z., Mai, H., Makhmutov, V., Manninen, H. E., Marten, R., Mathot, S., Mauldin, R. L., Nie, W., Onnela, A., Partoll, E., Petäjä, T., Pfeifer, J., Pospisilova, V., Quéléver, L. L. J., Rissanen, M., Schobesberger, S., Schuchmann, S., Stozhkov, Y., Tauber, C., Tham, Y. J., Tomé, A., Vazquez-Pufleau, M., Wagner, A. C., Wagner, R., Wang, Y., Weitz, L., Wimmer, D., Wu, Y., Yan, C., Ye, P., Ye, Q., Zha, Q., Zhou, X., Amorim, A., Carslaw, K., Curtius, J., Hansel, A., Volkamer, R., Winkler, P. M., Flagan, R. C., Kulmala, M., Worsnop, D. R., Kirkby, J., Donahue, N. M., Baltensperger, U., El Haddad, I., and Dommen, J.: The driving factors of new particle formation and growth in the polluted boundary layer, *ACP*, 21, 14275-14291, 10.5194/acp-21-14275-2021, 2021.
- 1100 Yan, C., Yin, R., Lu, Y., Dada, L., Yang, D., Fu, Y., Kontkanen, J., Deng, C., Garmash, O., Ruan, J., Baalbaki, R., Schervish, M., Cai, R., Bloss, M., Chan, T., Chen, T., Chen, Q., Chen, X., Chen, Y., Chu, B., Dällenbach, K., Foreback, B., He, X., Heikkinen, L., Jokinen, T., Junninen, H., Kangasluoma, J., Kokkonen, T., Kurppa, M., Lehtipalo, K., Li, H., Li, H., Li, X., Liu, Y., Ma, Q., Paasonen, P., Rantala, P., Pileci, R. E., Rusanen, A., Sarnela, N., Simonen, P., Wang, S., Wang, W., Wang, Y., Xue, M., Yang, G., Yao, L., Zhou, Y., Kujansuu, J., Petäjä, T., Nie, W., Ma, Y., Ge, M., He, H., Donahue, N. M., Worsnop, D. R., Veli-Matti, K., Wang, L., Liu, Y., Zheng, J., Kulmala, M., Jiang, J., and Bianchi, F.: The Synergistic Role of Sulfuric Acid, Bases, and Oxidized Organics Governing New-Particle Formation in Beijing, *GRL*, 48, 10.1029/2020gl091944, 2021.
- 1110 Yang, L., Nie, W., Liu, Y., Xu, Z., Xiao, M., Qi, X., Li, Y., Wang, R., Zou, J., Paasonen, P., Yan, C., Xu, Z., Wang, J., Zhou, C., Yuan, J., Sun, J., Chi, X., Kerminen, V. M., Kulmala, M., and Ding, A.: Toward Building a Physical Proxy for Gas-Phase Sulfuric Acid Concentration Based on Its Budget Analysis in Polluted Yangtze River Delta, East China, *EST*, 55, 6665-6676, 10.1021/acs.est.1c00738, 2021.
- 1115



- Yang, X., Xiao, D., Bai, H., Tang, J., and Wang, W.: Spatiotemporal Distributions of PM_{2.5} Concentrations in the Beijing–Tianjin–Hebei Region From 2013 to 2020, *Frontiers in Environmental Science*, 10, 10.3389/fenvs.2022.842237, 2022.
- 1120 Yao, L., Garmash, O., Bianchi, F., Zheng, J., Yan, C., Kontkanen, J., Junninen, H., Mazon, S. B., Ehn, M., Paasonen, P., Sipilä, M., Wang, M., Wang, X., Xiao, S., Chen, H., Lu, Y., Zhang, B., Wang, D., Fu, Q., Geng, F., Li, L., Wang, H., Qiao, L., Yang, X., Chen, J., Kerminen, V. M., Petäjä, T., Worsnop, D. R., Kulmala, M., and Wang, L.: Atmospheric new particle formation from sulfuric acid and amines in a Chinese megacity, *Science*, 361, 278–281, 10.1126/science.aao4839, 2018.
- 1125 Yokouchi, Y., Nojiri, Y., Toom-Saunty, D., Fraser, P., Inuzuka, Y., Tanimoto, H., Nara, H., Murakami, R., and Mukai, H.: Long-term variation of atmospheric methyl iodide and its link to global environmental change, *GRL*, 39, n/a–n/a, 10.1029/2012gl053695, 2012.
- Yokouchi, Y., Osada, K., Wada, M., Hasebe, F., Agama, M., Murakami, R., Mukai, H., Nojiri, Y., Inuzuka, Y., Toom-Saunty, D., and Fraser, P.: Global distribution and seasonal concentration change of methyl iodide in the atmosphere, *Journal of Geophysical Research*, 113, 10.1029/2008jd009861, 2008.
- 1130 Zhang, R., Xie, H. B., Ma, F., Chen, J., Iyer, S., Simon, M., Heinritzi, M., Shen, J., Tham, Y. J., Kurtén, T., Worsnop, D. R., Kirkby, J., Curtius, J., Sipilä, M., Kulmala, M., and He, X. C.: Critical Role of Iodous Acid in Neutral Iodine Oxoacid Nucleation, *Environ Sci Technol*, 56, 14166–14177, 10.1021/acs.est.2c04328, 2022.
- 1135 Zhou, Y., Hakala, S., Yan, C., Gao, Y., Yao, X., Chu, B., Chan, T., Kangasluoma, J., Gani, S., Kontkanen, J., Paasonen, P., Liu, Y., Petäjä, T., Kulmala, M., and Dada, L.: Measurement report: New particle formation characteristics at an urban and a mountain station in northern China, *ACP*, 21, 17885–17906, 10.5194/acp-21-17885-2021, 2021.

1140



Data availability. Measurement data at the AHL/BUCT and SORPES station, including acids concentration data, trace gas and aerosol data and meteorological data, are available upon request from the corresponding authors before the relevant databases are open to the public.

1145

Author contributions. WN and XCH designed the research. YZ, CD, YG, YL, CH, TL and ZW conducted the measurements at the AHL/BUCT station. DL, YL, CL, LC, YL, LW and XC conducted the measurements at the SORPES station. YZ, DL, XCH, WN, CD, RC, YL, YG, TP, FB, XQ, PP, YL, CY, JJ, AD and MK analyzed the data and interpreted the results. YZ, DL, XCH and WN prepared the manuscript with contributions from all co-authors.

1150

Competing interests. The authors have no competing interests to declare.

Acknowledgements. We thank colleagues and students at the AHL/BUCT station and the SORPES station for their contributions to the maintenance of the measurements.

1155

Financial support. This work was supported by the National Natural Science Foundation of China (NSFC) project (92044301, 42220104006, 42075101 and 41975154), the Jiangsu Provincial Collaborative Innovation Center of Climate Change and the Fundamental Research Funds for the Central Universities. Financial support from Samsung PM2.5 SRP is also acknowledged.

1160